Institute of Paper Science and Technology

FUNDAMENTALS OF INTERNAL STRENGTH ENHANCEMENT
PART TWO: STUDIES ON THE BONDING OF SINGLE FIBERS

Project 3526

Report 3

to

MEMBER COMPANIES OF THE INSTITUTE OF PAPER SCIENCE AND TECHNOLOGY

July 1992

Atlanta, Georgia

INSTITUTE OF PAPER SCIENCE AND TECHNOLOGY

Atlanta, Georgia

FUNDAMENTALS OF INTERNAL STRENGTH ENHANCEMENT PART TWO: STUDIES ON THE BONDING OF SINGLE FIBERS

Project 3526

Report 3

A Progress Report

to

MEMBER COMPANIES OF THE INSTITUTE OF PAPER SCIENCE AND TECHNOLOGY

By

Robert A. Stratton

July 1992

TABLE OF CONTENTS

ABSTRACT

Bonding between wood pulp fibers is essential for paper sheet strength. Yet the understanding of the fiber/fiber bond and its dependence on fiber properties, the environment, and the presence of strength aids is inadequate. This study was designed to provide new information on the characteristics of bonding in paper by examining in detail the individual fiber/fiber bond. As well as quantitative measurements of the bond strength and its dependence on pulp, furnish, and relative humidity, we also examined the locus of failure of the bond using the scanning electron microscope.

Individual fiber/fiber bonds were formed from unbleached kraft or TMP pulps. Bond area was measured by the vertical polarized light technique of Page. A new, highly-sensitive fiber load elongation recorder (FLER 2) was developed to measure the bond breaking load. Scanning electron microscope (SEM) examination of the formerly-bonded fiber surfaces revealed the extent of wall damage. The damage was given a (subjective) ranking, and the presence or absence of additional S1 material along the edge of the bonded area was noted. Between 40 and 50 bonds from each pulp were tested to achieve a valid mean bond strength and information about its distribution. Either of two polymeric strength aid systems, one forming covalent bonds and one forming only ionic bonds, was used to enhance the bond strength for some pulps.

Bonds formed from latewood fibers were found to have about three times the bond strength (breaking load/bond area) of earlywood fibers in agreement with some earlier workers. Fiber wall damage of the formerly-bonded latewood fibers was also greater than for the earlywood samples. Refining had no significant effect on the bond strength. The strength aids provided about a twofold increase in the bond strength with concomitant increase in the amount of fiber wall damage. The TMP pulp produced surprisingly strong bonds, although SEM examination gave no evidence of adhesive (lignin and hemicellulose) flow. These bonds were further enhanced when a strength aid was included. The decrease in bond strength with increasing relative humidity for an unbleached kraft pulp paralleled the decrease in tensile strength and modulus of handsheets tested under those conditions.

The fiber wall damage produced during bond failure varied greatly from one fiber pair to the next but, in general, increased with increasing bond strength. The torn S1 material along the edges of the bonded area was interpreted to be evidence of Nanko and Ohsawa's "skirt" effect. The presence of such material correlated with greater bond strengths thereby supporting the suggestion of those authors that the skirt should reduce the stress concentration present at the periphery of the bonded area.

Weak bonds tend to fail at the interface between the two fibers. Stronger bonds and particularly those that are enhanced with a polymeric strength aid shift the locus of failure to between the S1 and S2 layers of one (or both) fibers.

INTRODUCTION

The objective of this project is to provide a better understanding of the mechanism(s) of bonding in paper and in how these are enhanced by the addition of polymeric strength aids. In Progress Reports One and Two of this project (1, 2), the effects of a wide variety of chemical additives on sheet physical properties were studied using standard handsheet formation. The additives which were effective improved the properties of both chemical (bleached and unbleached) and mechanical pulps and under both acid and alkaline papermaking conditions.

Progress Report Three is concerned with an examination of the individual fiber/fiber bond. The purpose was to separate the effects of this elemental feature from those which depend on sheet structure (e.g., formation and relative bonded area) and individual fiber strength. These other factors will be the subject of the succeeding progress report. The current understanding of the mechanisms of bonding in paper, both with and without additives, was reviewed in Progress Report One and will not be repeated here.

BACKGROUND

The strength of a sheet of paper with randomly oriented fibers has been shown both theoretically (3, 4) and experimentally (5) to depend on two factors. These are 1) the strength of the individual fibers and 2) the strength and the number of bonds between them. Page et al. (6) have reviewed the earlier work on the strength of single fibers and have also shown that the strength is primarily dependent upon the fibril angle in the S2 layer and on fiber defects. Using larger fiber populations, Hardacker and Brezinski (7) showed that the fiber strengths of a given pulp had appoximately log-normal distributions with large coefficients of variation. They suggested that it may be necessary to include information about the distribution of fiber strength as well as its average value in correlations with sheet strength.

A specific objective of this project is to improve the strength of the individual fiber/fiber bond. This bond depends upon (a) the strength of the interaction between the two fibers and (b) the area over which these interactions occur (or the bonded area). In the absence of additives the interactions are thought to be hydrogen bonds plus the ubiquitous van der Waals bonds. Chemical additives can supplement these interactions to produce improved wet or dry strength. If the fiber/fiber interactions are strong enough, the locus of failure may be shifted from between the two fibers to between the S1 and S2 layers of one of the fibers. It is important that we know the location of the failure so that we may direct the chemical additives to this weak spot (i.e., between or within the fibers).

The bond shear strength of individual fiber bonds has been measured by a number of workers (8-17). They have investigated the effects of springwood vs. summerwood (9, 10, 12, 17), refining (8, 14), and yield (9, 12-14) sometimes with contradictory conclusions. Bonds were formed either between two fibers (8-12, 17), between a fiber and a shive of the same material (9, 16), or between a fiber and a cellophane strip (12-15). Sensitive instruments were constructed to measure the maximum load at failure. Bond areas were assumed to be either the total area of fiber overlap (10, 12-17) or the area in optical contact (8, 9, 11) as determined by the technique of Page et al. (18-20). Bond shear strength was then the ratio of the failure load to the bonded area. Values for the latter obtained by the various workers for a variety of species, pulping methods, and yields generally ranged from 3 to 5 MPa. A review of these measurements and others has recently been given by Uesaka (21).

The work discussed here is a continuation of that described above. Our main objective was to assess the effect of polymeric strength additives on bond strength. Because of their large size, these materials are precluded from entering the cell walls. In the small amounts typically used (1-2% based on the pulp), they have a negligible effect on the tensile strength of the individual fibers (11, 22). Although the ability of such material to improve sheet strength is widely appreciated and used commercially, Russell et al. (11) found no increase in fiber/fiber bond strength when the fibers were treated with either a melamine-formaldehyde resin or a polyamide polyamine epichlorohydrin resin. In view of the theories of paper strength (3, 4), we decided to look more closely at these interactions. In addition,we reexamined the effect of springwood vs. summerwood and refining on bond strength. Because good performance under conditions of high relative humidity is frequently an important paper and board property, we also studied the influence of this parameter on bond strength.

EXPERIMENTAL

Materials

Small sections of earlywood and latewood from loblolly pine were separately pulped using a conventional kraft cook. Following pulping and washing, the sections were gently defibered and stored at low consistency (23).

For most of this work, a conventional kraft cook of southern pine chips to a 47.5% yield (kappa number of 34.2) was used. The pulp was refined in a Valley beater to 570 and 345 mL CSF. The beaten pulps were classified in a Britt jar using a 65 mesh bronze wire to remove the fines. Distilled water was washed through the fibers until the filtrate was visually free of fines.

As a representative mechanical pulp a western hemlock thermomechanical pulp (TMP) was used. It was refined for 10 minutes in a Valley beater and classified by two passes over the Institute's web former.

All pulps were stored in the never-dried condition until used for fiber/fiber bond formation.

To study the effect of chemical additives on bond strength, we used either of the following combinations:

A/C - polyamide polyamine epichlorohydrin (PAE - 1% based on pulp) followed by carboxymethylcellulose (CMC - 0.4%). Espy (24) and our previous work (1) have shown that this ratio of the two polymers provides maximum sheet strength. The two polymers are cationic and anionic, respectively, and were added to dilute suspensions of the fibers sequentially with adequate time for adsorption. Under these conditions, virtually all of the polymers are adsorbed (25). It has been shown (26, 27) that covalent bonds (ester) can be formed between the azetidinium groups on the PAE and carboxyl groups on either the fiber surface or the CMC.

D/S - polydiallyldimethyl ammonium chloride (0.5%) followed by sodium polystyrene sulfonate (0.5%). These two are highly charged cationic and anionic polymers, respectively, and are added to the fibers similarly to the A/C combination. Because of their chemical structure, the only interactions possible are ionic: either between the cationic "D" and ionized carboxyl groups on the fiber surface or between "D" and the sulfonate groups on "S."

The pH of the fiber suspensions was near neutral, and no other additives were present.

Techniques

To obtain better contrast between bonded and unbonded areas determined using the vertical illumination, polarized light scattering method (18-20), we followed Page's technique (18) and dyed a separate portion of each set of fibers with Chlorazol Black E (before polymer treatment).

Fiber/fiber bonds were formed as follows. A dyed and an undyed fiber (each from a batch of strength aid-treated fibers, if desired) were positioned at right angles to each other on a teflon-faced silicone rubber disc (Microsep F-138, Supelco Inc) under water. To ensure a 90^{o} crossing angle and to maintain the fibers in place during pressing/drying, four tabs were cut in the teflon film and were peeled up to allow the fiber to be placed under them. The completed mount with the two fibers in place is shown in Fig. 1 with the dyed fiber mounted first. A second disc was placed teflon face down on top of the fibers. The fiber pair was then dried in an oven at 105^{o} C for one hour under a nominal compressive pressure of 0.12 MPa. The actual load in the fiber crossing (bonding) area would be somewhat greater, but the softness of the teflon and

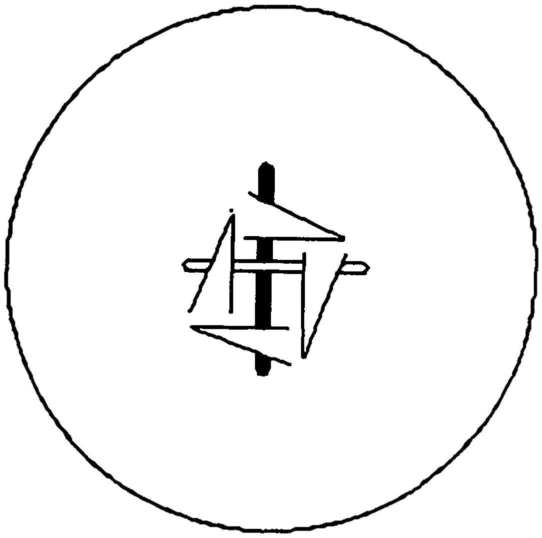

Fig. 1 Schematic representation of the teflon-faced septum modified to hold the fibers in place during pressing/drying.

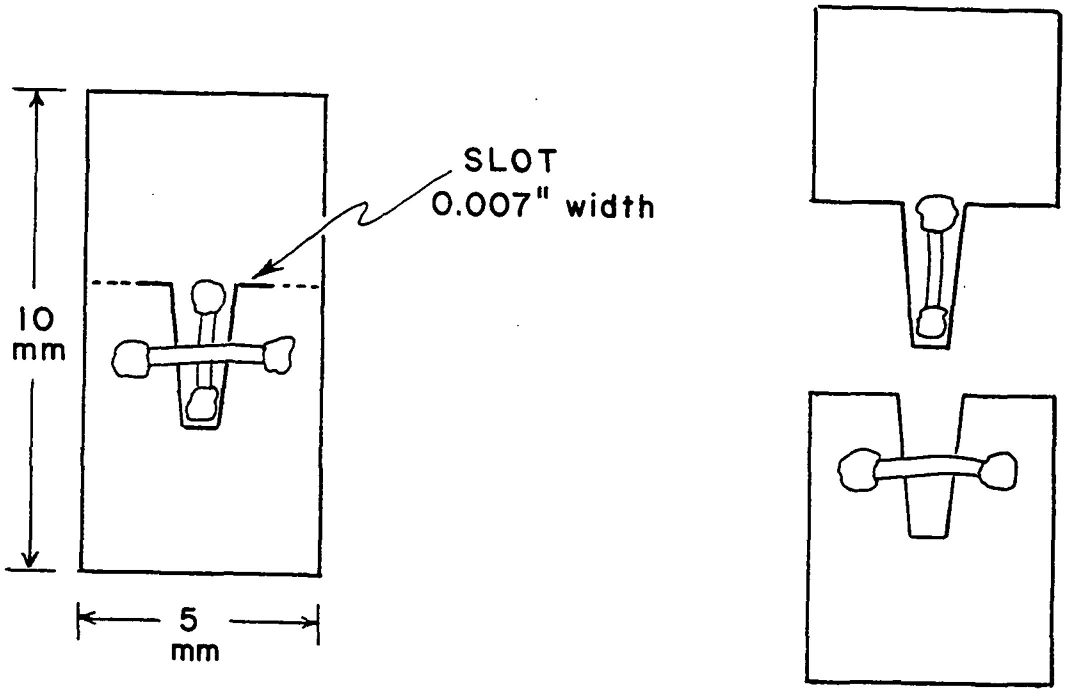

Fig. 2 Mylar tab for holding bonded fibers. a) Before bond fracture. b) After fracture.

rubber backing would tend to reduce the pressure. This arrangement amounted to drying under restraint and no evidence of shrinkage in the bonded regions was seen in subsequent scanning electron micrographs (SEM).

After drying, the now-bonded fiber pair was placed on a Mylar mount (Fig. 2) with the dyed fiber next to the mount and coaxial with the "tongue." The mount was fabricated from 0.010" thick Mylar by laser machining. The solid line in Fig. 2a is a 0.007" slot cut by the laser. Only the ends of the dyed fiber were glued to the Mylar at this time using Epon 907. (The drawing is to scale, except the fibers have been shown at about five times their real width for clarity.)

Both bond formation and bonded-fiber mounting were carried out under a binocular microscope.

The scattered light from the individual fiber/fiber bonds using Page's technique (18-20) was photographed. Slides (35mm) were prepared and projected. The bonded (dark) area was traced and its area determined using an Apple Graphics Tablet connected to an Apple II microcomputer. The system was calibrated using an area of known size to convert the (optically) bonded area to units of square micrometers. A typical example of a bond is shown in Fig. 3 along with the bonded area drawn from it. With crossed polarizers the dyed fiber is invisible. The tongue area of the mount was painted with black ink before the fibers were attached to it. This reduced reflection from the Mylar and enhanced the contrast between bonded and unbonded regions. Polaroid photographs of each bond were taken at the same time using both crossed and uncrossed polarizers.

After determination of the bonded area, the Mylar mount was installed in the sample clamps of the FLER 2. The latter is a second generation fiber-load-elongation-recorder (28) with increased sensitivity and versatility (see below). The parts of the Mylar mount shown as dotted lines in Fig. 2a were cut using a hot wire, and the ends of the undyed (cross) fiber were cemented to the female portion of the mount using a plasticized phenoxy hot melt (Thermogrip 1315). It was found necessary to delay the attachment of the cross fiber until this point; otherwise, cutting the mount with the hot wire produced enough deformation to the fiber/fiber bond to frequently cause its failure.

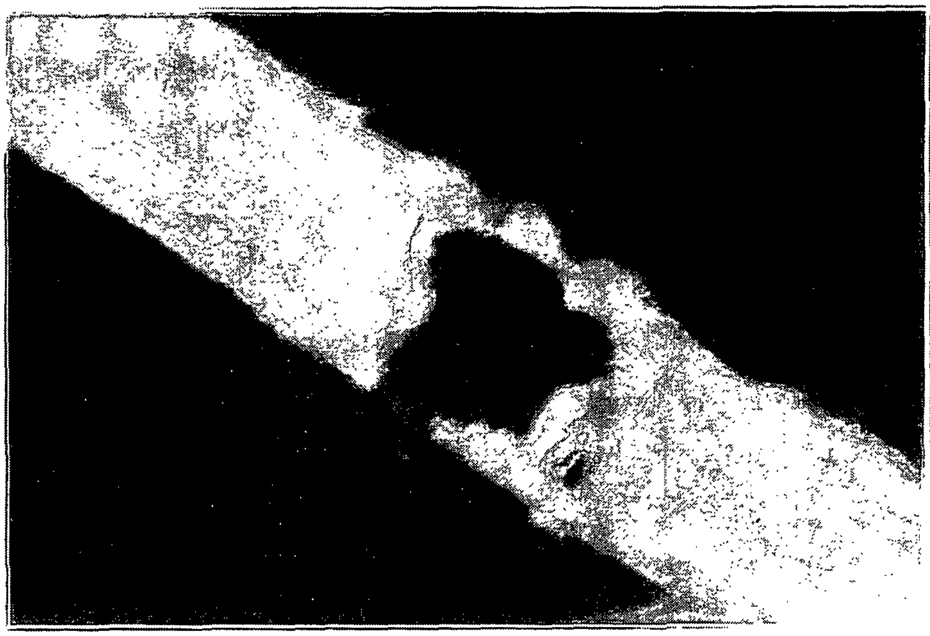

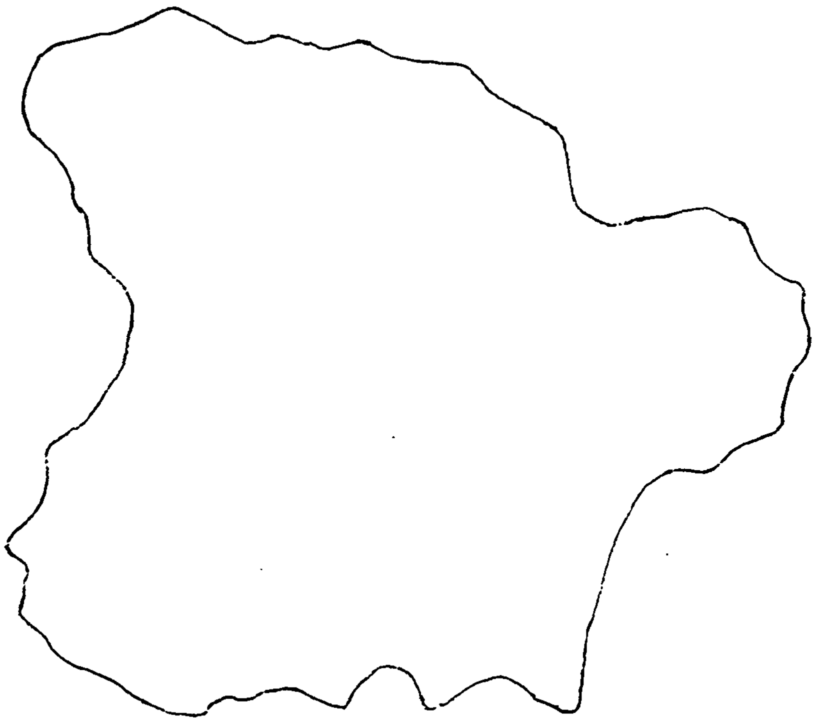

Fig. 3 a) Fiber/fiber bond viewed with polarized vertical illumination.
b) Outline of bonded area produced by tracing a projection of the negative print of a).

When the hot melt adhesive had hardened, the bond was strained to failure. The load at failure was recorded. Because the fibers are only attached to the mount at their ends, the bonded region is free to rotate out of the plane, and the stress geometry is not plane shear but contains a peeling component. Observation of the bond with a binocuar microscope during straining revealed only a catastrophic failure. Partial debonding for stresses lower than the ultimate did not occur.

The FLER 2 was located in a room with the atmosphere controlled at 23^{o} C and 50% RH, and the tests were made at those conditions except as noted below.

After bond failure the two parts of the Mylar mount each with its attached fiber (Fig. 2b) were removed from the clamps of the FLER 2, coated with gold-palladium in vacuo, and installed in a scanning electron microscope. Formerly-bonded areas were easily recognized, and the locus of failure could be seen (25).

For comparison purposes, a (subjective) rating of the degree of damage in the formerly-bonded area was devised and is shown in Fig. 4. The failure surface of each of the formerly-bonded fibers (axial and cross) was compared with those in Fig. 4 and assigned a ranking of 1 to 6. Briefly, the relative amounts of damage for the six archetypes in Fig. 4 can be described as follows.

1. No damage.
2. Slight "picking" of the surface.
3. Moderate "picking."
4. Significant "picking," some tearing of surface layer.
5. Moderate tearing.
6. Extreme tearing.

Note that the background in archetypes 2, 4, and 6 (which are axial or "tongue" specimens) is the inked surface of the Mylar mount.

For those fibers that had been refined, additional damage to their surfaces was sometimes evident and took the form of external fibrillation and peeling of wall material at the edges of the fibers. This type of damage is exhibited by the prototypes in Fig. 4 and was assigned a "Damage Type" of unity. The unrefined

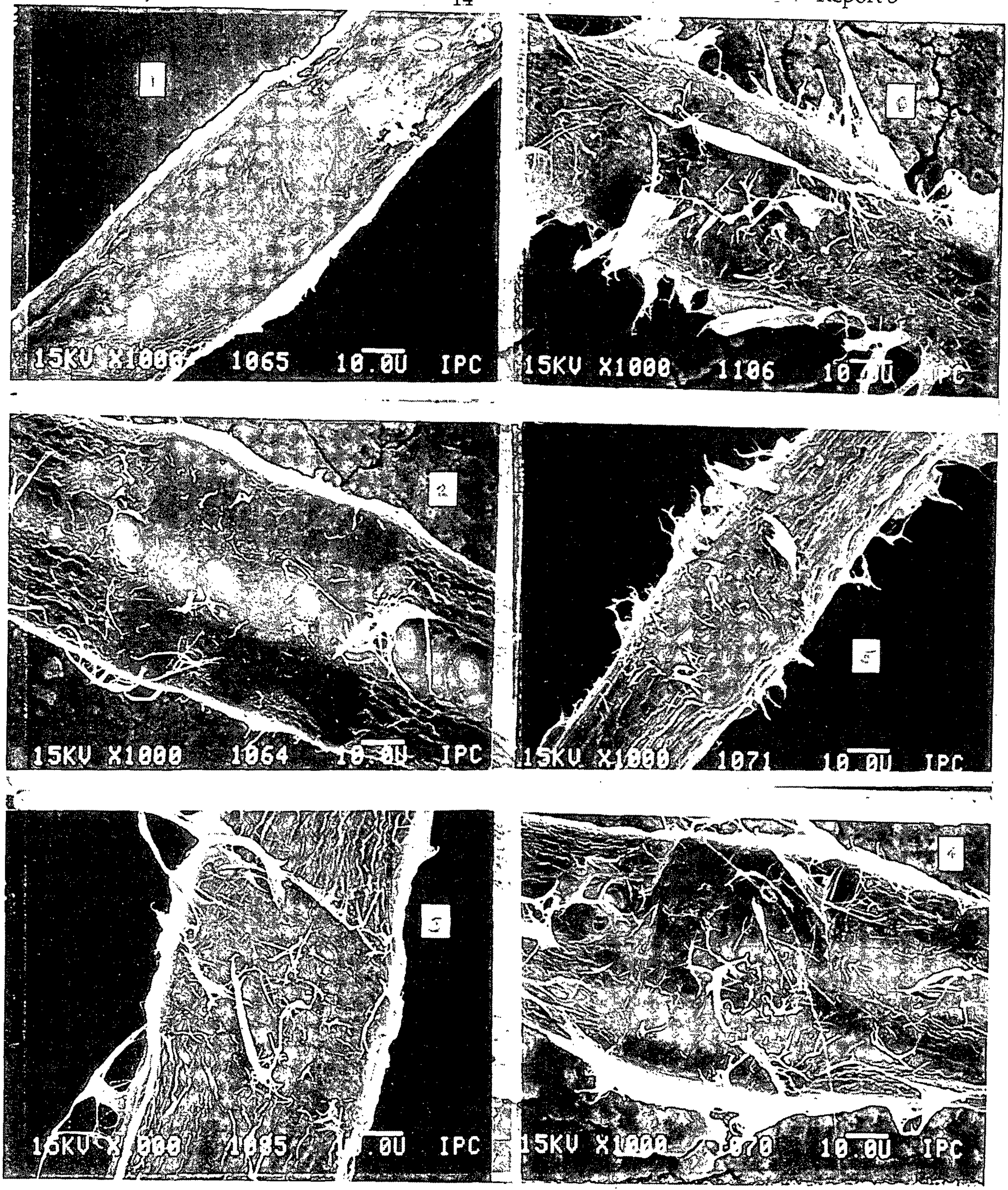

Fig. 4 Archetypes of fiber damage resulting from bond rupture. Increasing rank from 1 to 6 anticlockwise starting in upper left-hand corner.

fibers and some of the refined fibers showed no such damage and were given a value of zero for this parameter. The presence or absence of this material along the edges of the fiber appeared to be independent of the amount of damage in the central portion of the bond.

FLER 2

Rather than try to upgrade the FLER 1, it was decided to design and construct a versatile new instrument with adequate range and sensitivity. Keith W. Hardacker designed and supervised the construction of the new instrument (29) which is shown in Fig. 5.

The core of the instrument is the specimen handling system in the right-hand side of the photo. A schematic of this is shown in Fig. 6, where an electronic weighing cell, A, is suspended beneath a mounting plate, B, by means of four flexure springs, C (Fig. 7). A dc servo motor, D, turns a differential screw, E, pulling or pushing the weighing cell to apply a tensile or compression load to a specimen mounted between the clamps, F. The right-hand clamp may be positioned along the test axis by the compound microscope focusing mechanism, G, and be locked in place by the clamp, H. Specimen extension or compression is measured between this fixed clamp and the opposing, movable clamp. A capacitive displacement transducer, I, supported by the pillar, J, senses the position of the movable clamp.

The signal for driving the dc motor is derived by comparing the signal from the load or elongation sensor with a linear ramp reference voltage. Thus, testing may be done either at constant rate of loading or constant rate of elongation. The ramp generator (at the bottom of the rack in Fig. 5) supplies the ramp and the necessary controls for varying the rate at which the tensile or compression test is performed and setting the load or elongation limits between which the loading and unloading may be cycled.

Two different load cells and two different elongation sensors can be used to provide a wide range of infinitely adjustable load and deformation rates. These are listed in Table 1.

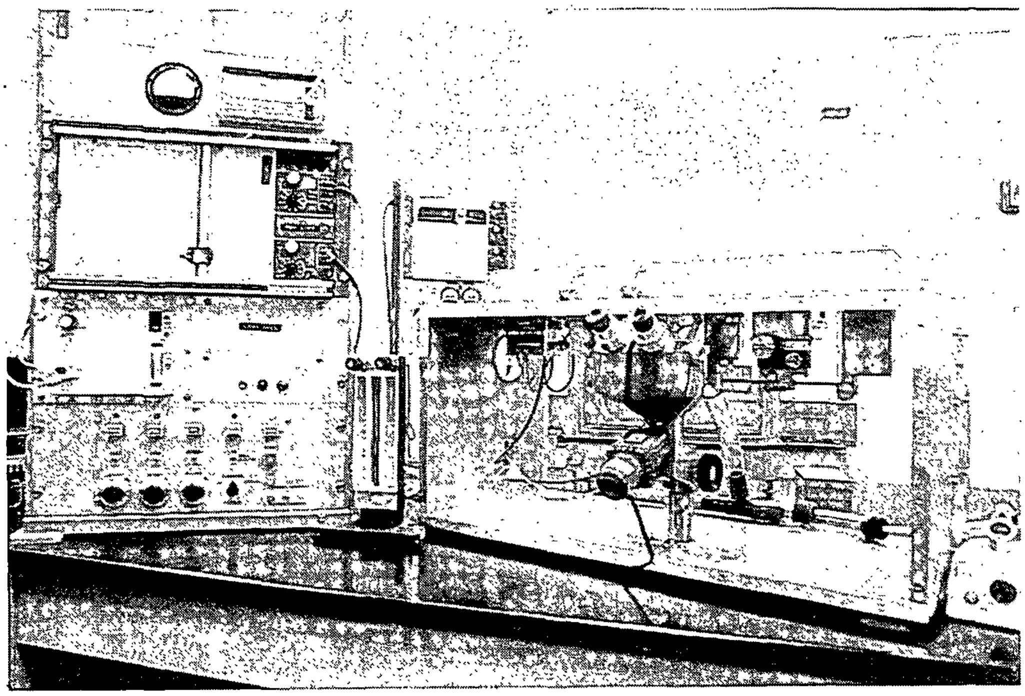

Fig. 5 Photograph of FLER 2.

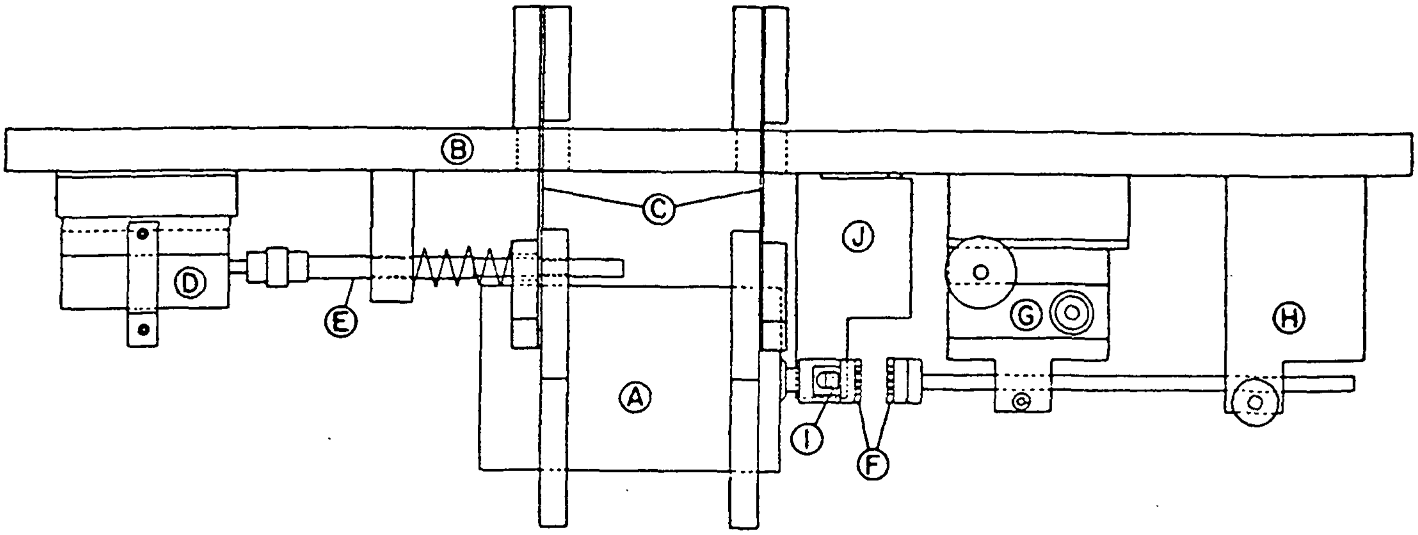

Fig. 6 Side view of FLER 2.

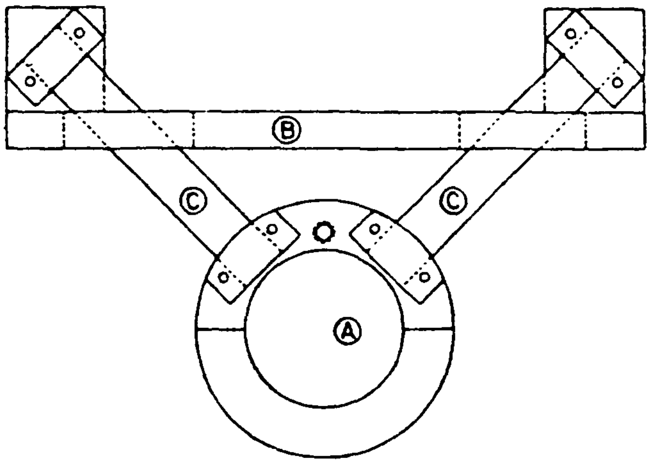

Fig. 7 End view of the mounting structure for the load cell of the FLER 2.

Table 1. Measurement Ranges of FLER 2.

Elongation cell I	(0.05 mm range, 0.05 µm sensitivity) 0.026 µm/sec to 15 µm/sec
Elongation cell II	(0.25 mm range, 0.25 µm sensitivity) 0.13 µm/sec to 74 µm/sec
Load cell I	(50 g range, 1 mg sensitivity) 0.05 g/sec to 30 g/sec
Load cell II	(400 g range, 5 mg sensitivity) 0.42 g/sec to 242 g/sec

The measured load and elongation signals are applied to an x-y recorder mounted on the rack. They may, of course, also be fed to a digital processor when appropriate. Use of other reference waveforms is also possible, if desired, e.g., logarithmic rate change , hold at constant load or elongation, sine wave cycling, rate proportional to measured work input, etc.

A stereoscopic microscope is mounted to permit viewing and/or photographing of the specimens during mounting and testing.

It is desirable to conduct fiber and bond tests at various moisture contents. This necessitates immersing the specimens in various relative humidity atmospheres by (a) placing the apparatus in suitably conditioned rooms, (b) conditioning the interior of a box containing the apparatus, or (c) bathing the specimen in a gentle stream of conditioned air. For the present work, alternatives (a) and (c) were implemented. The insturment was located in a 50% RH, 23^{o} C room. Sample moisture content, at 23^{o} C, was varied by passing air conditioned to other relative humidities over the specimen. This custom-conditioned air was produced by mixing dry air from a tank of compressed, dry air with moisture-saturated air produced with a small bubble-type saturation. A schematic of the system is shown in Fig. 8, and a photographic close-up of the sample area of the FLER 2 with the conditioned air being transported by the plastic tube is given in Fig. 9. The air flow rates required are low enough and the moisture equilibration

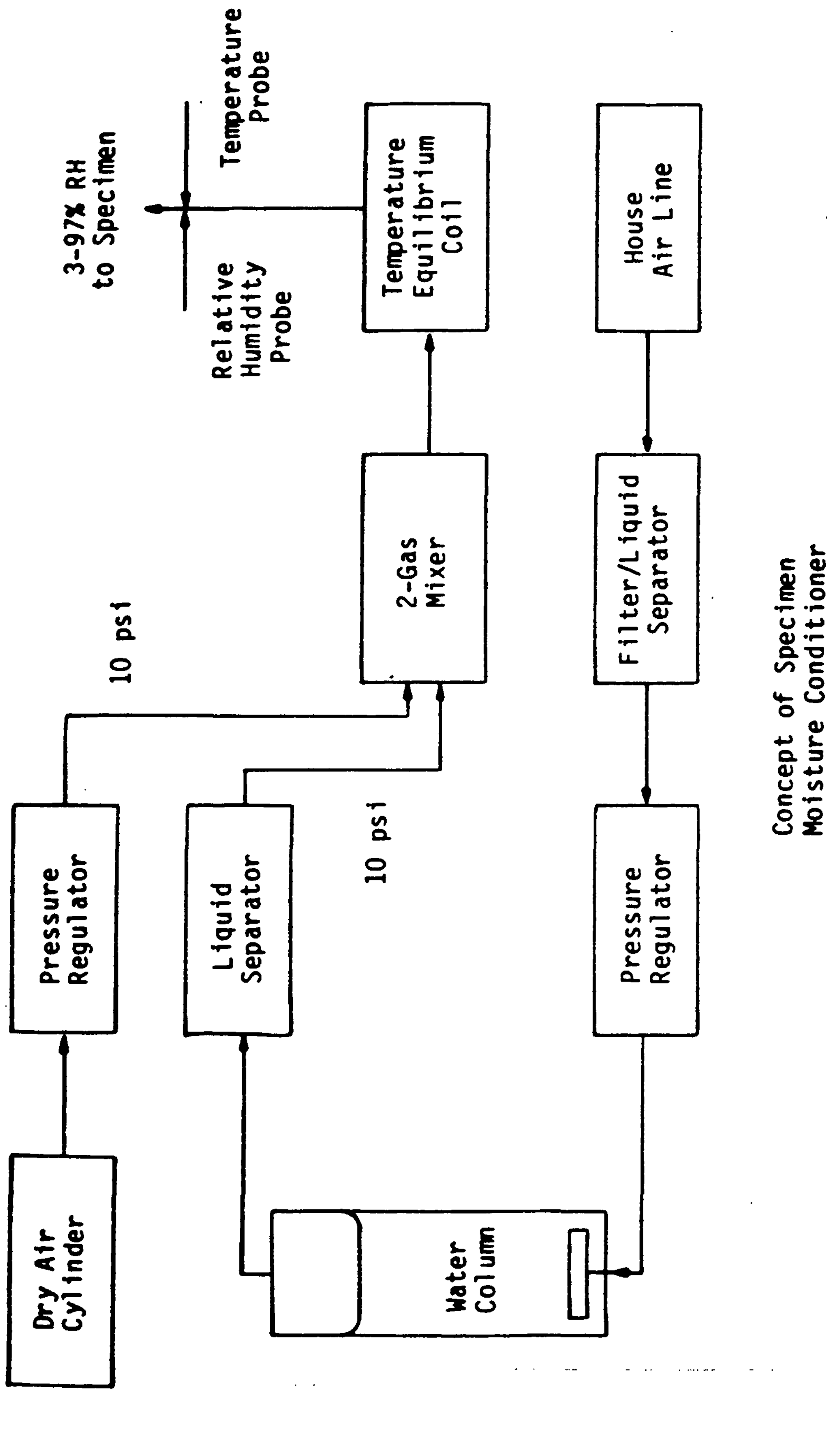

Fig. 8 Schematic of the specimen moisture conditioner.

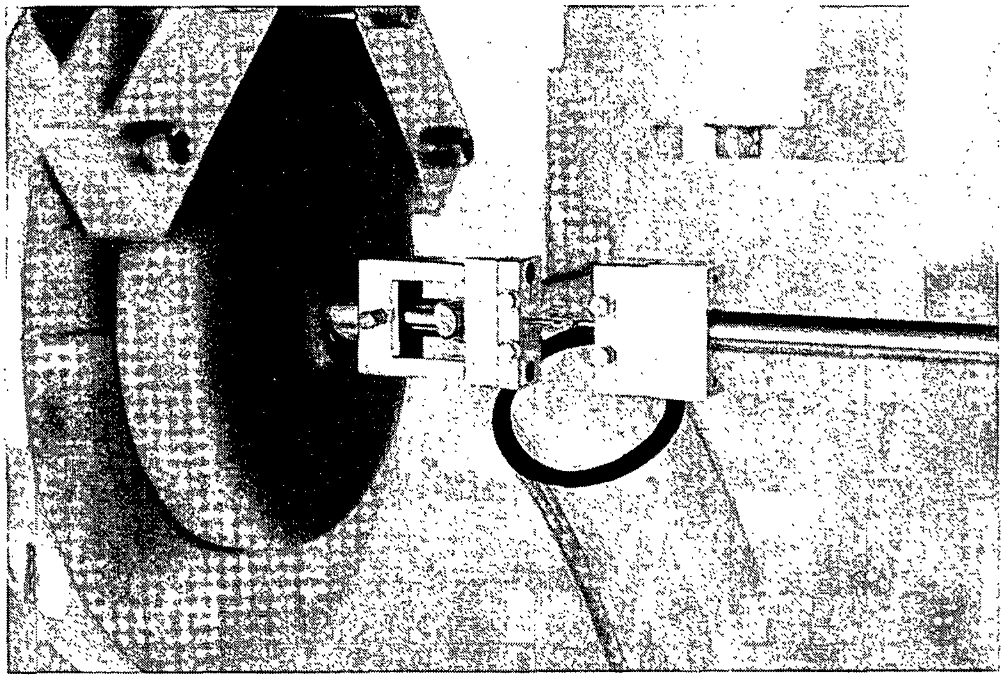

Fig. 9 Close-up view of the specimen area of the FLER 2.

rates of single fibers are fast enough to make this a practical, relatively inexpensive process, while also providing maximum ease of access to the test area. Temperature and relative humidity are sensed by a probe near the specimen and are displayed on a readout at the top of the equipment rack in Fig. 5.

If it is desired at some later time to test at other temperatures, it would probably be best to supply larger quantities of conditioned air to the box-like support structure of the apparatus. This air might best be provided by a commercial, mechanically-refrigerated, air handling unit.

For the bond strength measurements reported here, bond breaking loads were less than 10 grams and were accurately measured by the FLER 2. Because the cross fiber was bonded to the mount near its ends, the deformation produced during a test was a sum of that of the fiber (bending) and the bond. The contribution of the latter was minor, and therefore, the work to rupture the bond could not be determined.

RESULTS AND DISCUSSION

BOND STRENGTH

Distribution of Values

The complete data for all the samples are listed in the Appendix. The mean values of the bond breaking load, bonded area, and their ratio (load/area), the bond strength, are given in Table 2 for the various samples. Between 40 and 50 bonds were tested for each sample, and the standard deviations of the three properties are given in parentheses in the table. The large standard deviations are likely a result of several factors: 1. The inherent variability of the fibers themselves (7). Nordman and Qvickstrom (30) showed that the tensile breaking load of fibers taken from a narrow position within a growth ring exhibited low variability. The present fibers were either from throughout an earlywood or

Table 2. Mean Fiber Bond Properties

Fiber	Code	Additives [a]	R.H., %	Breaking Load, g	Bond Area, μm^2	Bond Strength, MPa
Earlywood	E0	--	50	0.47 (0.48) [b]	2410 (840)	2.1 (2.1)
Latewood	L0	--	50	0.87 (0.56)	1500 (540)	6.4 (4.2)
Earlywood	EAC	A/C	50	1.14 (0.48)	3000 (770)	3.9 (1.7)
570 mL CSF	A5	--	50	0.73 (0.65)	2070 (720)	3.5 (2.8)
570 mL CSF	A75	--	75	0.60 (0.47)	2260 (810)	2.9 (2.4)
570 mL CSF	A88	--	88	0.42 (0.32)	2220 (820)	2.1 (1.9)
570 mL CSF	AAC	A/C	50	1.44 (1.22)	2130 (800)	7.5 (6.7)
570 mL CSF	ADS	D/S	50	1.51 (0.92)	2040 (740)	9.3 (5.7)
345 mL CSF	A3	--	50	0.68 (0.48)	2290 (1070)	3.7 (4.4)
TMP	T0	--	50	0.40 (0.36)	760 (560)	7.9 (8.9)
TMP	TAC	A/C	50	1.28 (0.86)	1620 (770)	10.2 (10.7)

a) Fibers treated with A/C (see text) or D/S polymers.

b) Values in parentheses are standard deviations.

latewood region or were a mixture of early and latewood. Thus, fiber wall thickness and fiber flexibility varied from fiber to fiber. For the beaten pulp, the effect of the refining probably varied along the length of a fiber as well as from fiber to fiber. 2. Morphological features (e.g., pits) will vary along a fiber and from fiber to fiber and will affect the intimacy of interfiber conformability and bonding. 3. The relative proportions of shear and peeling will vary from one bond to the next. A greater degree of peeling would be expected to lower the bond breaking load and the calculated bond strength.

In spite of the large variability (and standard deviation), the results are amenable to interpretation. Comparisons between samples for a particular property were tested using the t-statistic. In the following discussion, statements regarding either the inequality or the equality between two values can be made with a probability of their being valid of greater than 99%.

Representative results (probability plots) for breaking load, bonded area, and bond strength are shown in Figs.10-12 (for earlywood). Bond strength as noted previously (10) and load follow log normal, while bonded area follows a normal distribution. The results for the other samples also clearly follow these same distributions, although the scatter in some cases is greater. In contrast, Mohlin (12) found a normal distribution for the bond strength for cellulose fibers bonded to cellophane. Hardacker and Brezinski (7) have shown that the tensile breaking load of individual fibers follows a log normal distribution.

It would be expected that there would be a linear relationship between the load and the bonded area. In reality, there is not as is shown in Fig. 13, and the other comparable data given in detail in the literature (8, 16) also fail to show the expected trend. Likely, this is a result of one (or more) of the three factors leading to variability discussed above.

Button (17) has shown that cellophane strips apparently follow linear elastic fracture mechanics where breaking load <u>decreases</u> with increasing bond length due to stress concentration effects. Application of this concept to the present data

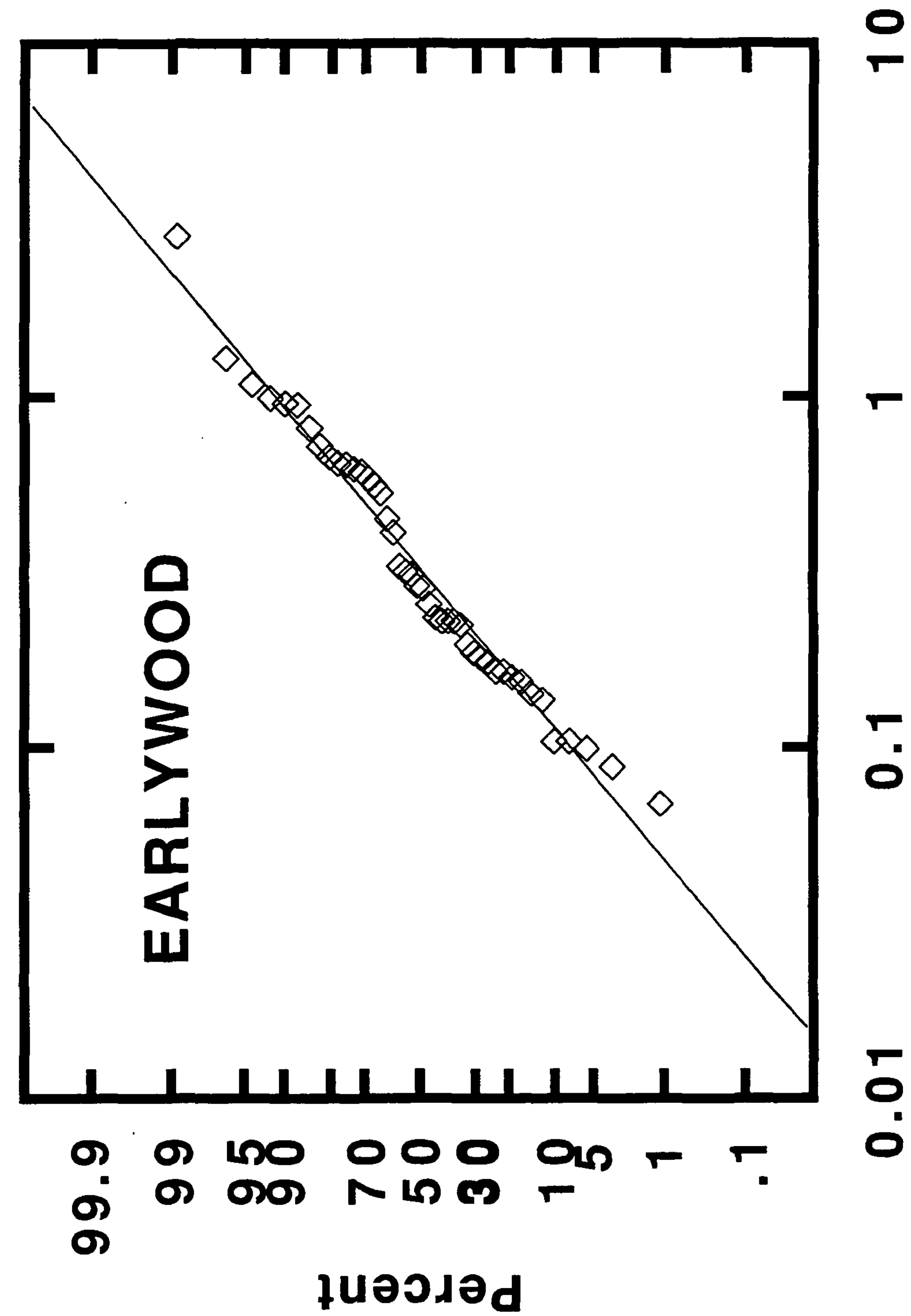

Fig. 10 Probability plot of bond breaking load for pulp E0 showing log normal distribution.

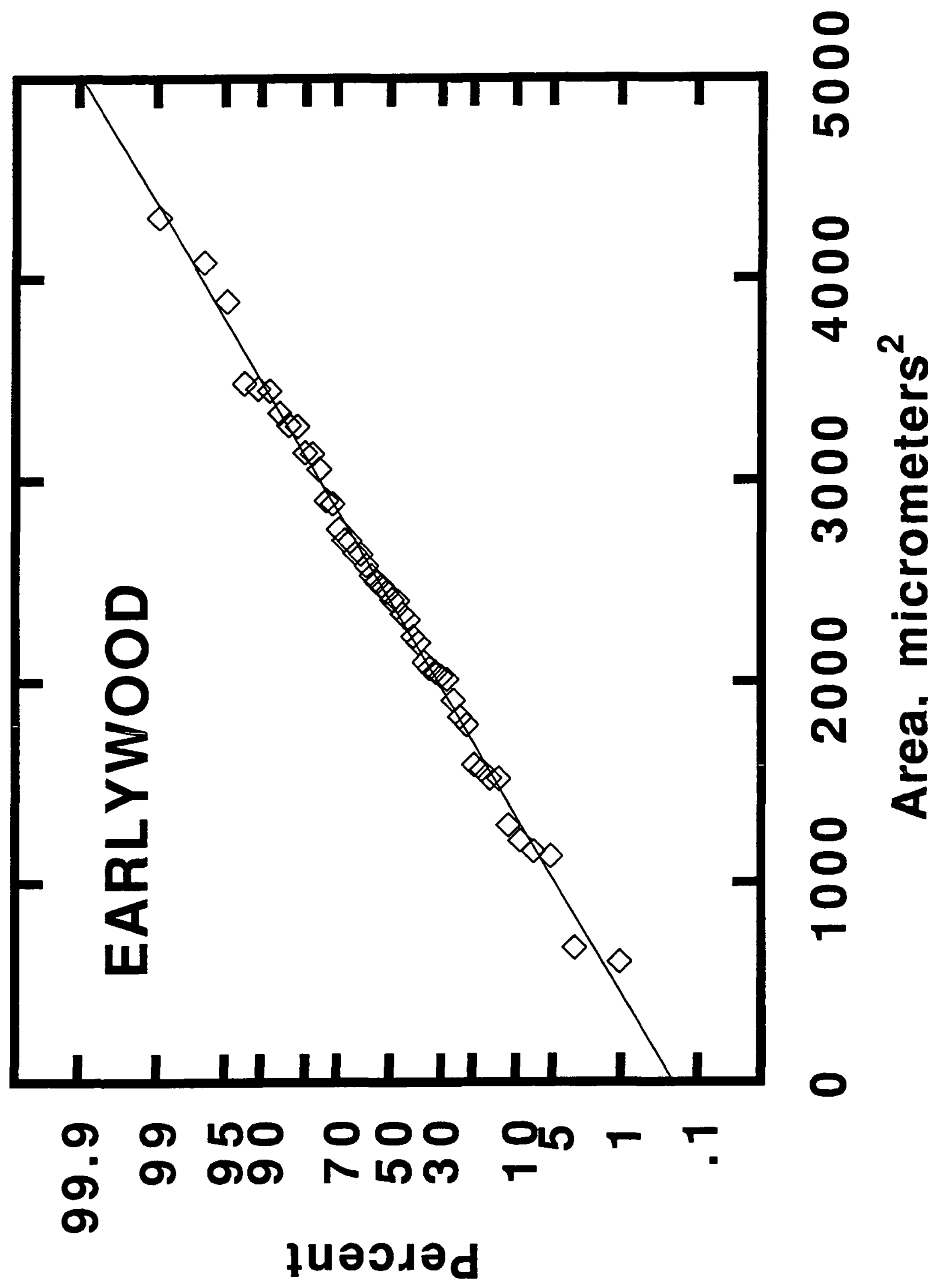

Fig. 11 Probability plot of bonded area for pulp E0 showing normal distribution.

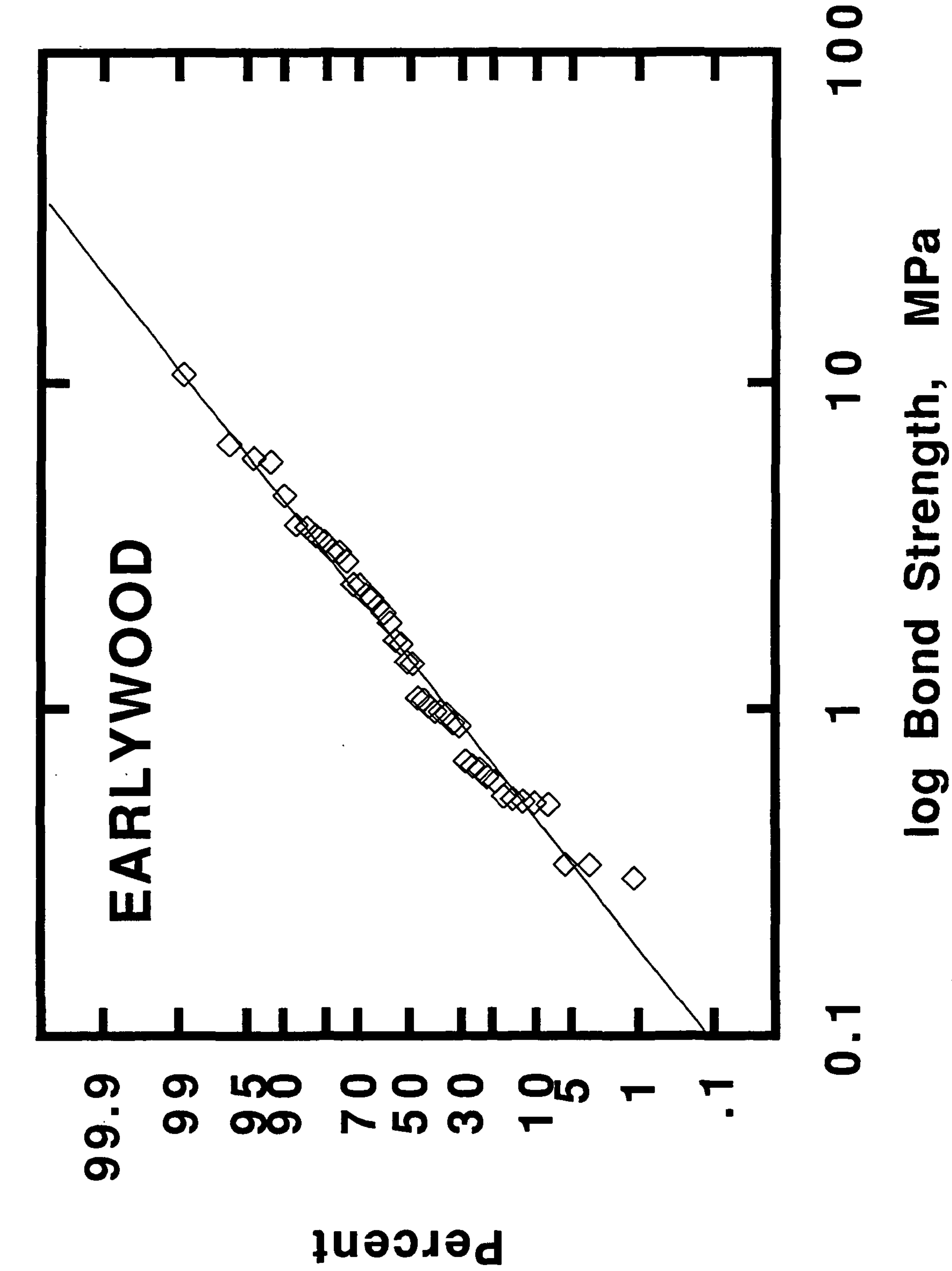

Fig. 12 Probability plot of bond strength for pulp E0 showing log normal distribution.

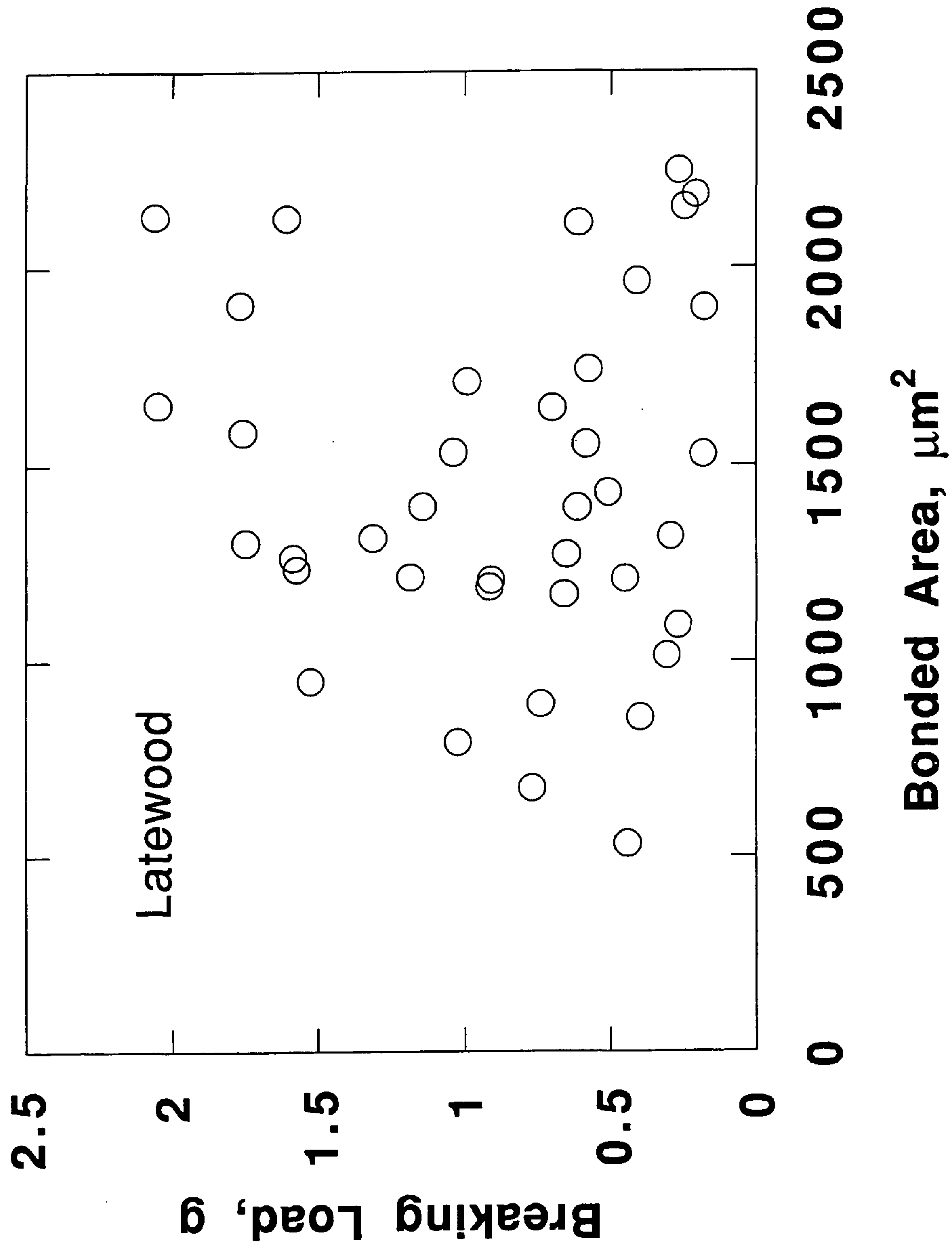

Fig. 13 Plot showing lack of correlation between bond breaking load and bonded area for pulp L0.

did not produce any clear trend, again perhaps due to the variable fiber population and strain geometry. (Also, see below.)

Earlywood vs. Latewood

Several workers (9, 10, 17) have shown latewood fiber bonds to have a higher strength than earlywood bonds. Mohlin (12), on the other hand, using fibers bonded to cellophane found no difference in strength between them for four different pulps. The present results (Table 3) show that, for both breaking load and bond strength, the latewood fibers are stronger. As expected for the thicker-walled, less conformable latewood fibers, their bonded area is much smaller. Mohlin (12) agrues that the bond strength is a function only of the surface chemistry of the fibers and therfore would be expected to be the same for early and latewood. Perhaps, the difference between her work and that of the other workers and the present study lies in the experimental geometry. The stress distribution in the case of a fiber/fiber bond would be expected to be influenced more by cell wall thickness than would the fiber/cellophane bond. The fiber/fiber bond geometry may be closer to the situation prevailing in a sheet of paper.

Table 3. Mean Bond Parameters of Earlywood and Latewood Fibers (Loblloly pine).

Fiber	Breaking Load, g	Bond Area, μm^2	Bond Strength, MPa
Earlywood	0.47	2400	2.1
Latewood	0.87	1500	6.4

Effect of Refining

In agreement with previous workers (8, 14), we find (Table 4) no statistically significant difference between the properties of bonds between fibers from pulps refined to 570 and 345 mL CSF. It may be that already at 570 mL CSF most of the

S1 layer has been removed, and bonding is primarily between the S2 layers of the two fibers, with a similar situation at 345 mL CSF. It could be argued that unrefined fibers with S1 intact might have different bonding properties. We do not have such a comparable sample, unfortunately. On the other hand, the load and bond strength for the refined samples fall between those for the unrefined earlywood and latewood (Table 3) as might be expected since they comprise a random sample of refined early- and latewood fibers. In fact, assuming a 55% latewood/45% earlywood composition for the lightly beaten sample (570 mL CSF) and that the properties are additive by weight fraction, values for breaking load, bond area, and bond strength that are within 10% of those measured can be calculated from the corresponding data for the separate components.

Page (3) tested his theory of sheet strength using the data of Ingmanson and Thode (31) for a bleached sulfite northern softwood pulp. From his analysis, Page concluded that the bond strength was independent of refining for samples of this pulp ranging from unbeaten to very highly beaten.

Table 4. Mean Bond Parameters for Refined Fibers (Unbleached kraft pine).

Refining, mL CSF	Breaking Load, g	Bond Area, μm^2	Bond Strength, MPa
570	0.73	2100	3.5
345	0.68	2300	3.7

Effect of Strength Aids

Comparison of the untreated and polymer-treated fiber is shown in Table 5. When the earlywood fibers are treated with A/C, all three bond properties increase. This disagrees with the results of Russell et al. (11) cited previously. The fact that a measurable increase in bonded area occurs may be attributed to the thin walls and great flexibility of earlywood fibers. Perhaps, the strength aid is effective here in reducing "springback" during drying which tends to decrease the bonded area.

For the refined pulp, both strength aid combinations (A/C and D/S) are equally effective in improving load and bond strength. As with the earlywood fibers, greatly enhanced bond strengths are produced. Here (perhaps, because the sample includes both early- and latewood), no change in bonded area is found. The fact that A/C and D/S produce comparable results is surprising. The former can interact with the cellulosic fibers via hydrogen, ionic, and covalent bonds, whereas the latter has only the possibility of ionic bonds. Evidently, covalent bonds are not necessary for high strength. These results confirm our previous work (1, 2) on the strength of handsheets when these additives are used. Although ionic bonds can provide only temporary wet strength, they have the advantage (over strength aids forming covalent bonds) of being readily repulpable. Such strength aids may find increased use in the near future in paper designed to be recycled. We have recently shown (32) that strength aids such as A/C and D/S can shift sheet strength from being bond strength-limited to being fiber strength-limited even with high-yield pulps.

Table 5. Effect of Strength Additives on Mean Bond Parameters.

Fiber	Additive	Breaking Load, g	Bond Area, μm^2	Bond Strength, MPa
Earlywood	None	0.47	2400	2.1
Earlywood	A/C	1.14	3000	3.9
570 mL CSF	None	0.73	2100	3.5
570 mL CSF	A/C	1.44	2100	7.5
570 mL CSF	D/S	1.51	2000	9.3

TMP

We found it very difficult to produce fiber/fiber bonds from these stiff fibers. Many failed to bond under our pressing and drying conditions, and many more were so weak that they failed during sample mounting. The breaking load is correspondingly low (Table 2). Because of the rather rigid character of these fibers, conformability and hence bond area is low. It is surprising then that the specific bond strength for this material is the highest of any (untreated) fibers that we have measured. The only other single fiber results in the literature for mechanical pulps are those of Thorpe et al. (16) for a Scotch pine TMP. They found that the strength depended strongly on the drying temperature used during bond formation. At 110° C the bond strength was 2.8 MPa, while at 210° C the strength was 8.1 MPa. For the latter case, they suggest that "a thermal flow of lignin and hemicelluloses may provide an adhesive matrix which infiltrates all layers of both the fiber and the shive cell walls, forming a continuum." The large value we find at a drying temperature of 105° C would appear to be at odds with these results. For their very strong bonds (210° C), they also found frequent fiber failure rather than bond failure and again attributed this to the very strong bond formed by the adhesive matrix. We did not find fiber failure, but this likely reflects our different experimental arrangement. While we used a single fiber/fiber bond, they bonded a single fiber to a number of others (shive) to produce a "large" bond whose strength was frequently greater than the fiber's axial tensile strength. Whether we had "adhesive" flow during sample preparation remains unresolved, but SEM evidence suggests we did not.

Despite the very strong bonds produced with the untreated TMP fibers, we were still able to enhance them more by the use of chemical additives (Table 2). Breaking load, bonded area, and bond strength were all increased when the polymers were added. This result agrees with our previous work on the effect of this additive combination on the strength of handsheets made from this pulp (2). Apparently, the polymers are able to interact with the lignin-rich surfaces of these fibers in much the same way as they do with the lower yield chemical pulps. The large increase in bonded area when the additives are present is unexplained.

Effect of Relative Humidity

It is well-known that both sheet and individual fiber properties are affected by the relative humidity (or moisture content). Specifically, both the tensile strength and the tensile modulus of these decrease with increasing relative humidity. Since sheet strength is a function of the properties of both the individual fibers and of the bonds between them, it was not evident whether the fiber/fiber bond was also influenced by moisture. Experiments were carried out, therefore, to ascertain this dependence on the lightly refined fibers (570 mL CSF). Individual fiber/fiber bonds were prepared as before. After installation in the FLER 2 for breaking load measurement, the bonded fibers were conditioned in a gentle stream of air regulated to either 75 or 88% RH. The conditioning period of three minutes at the elevated relative humidity was judged sufficient for the sample to essentially attain moisture equilibrium. The bond was then strained to failure as usual. The average strength values are listed in Table 6. Bond strength decreases with increasing relative humidity as do individual fiber strength and sheet strength.

It should be pointed out that the bond areas listed in Table 6 and used for the calculation of the bond strength values in that table were determined at 50% RH rather than at the indicated relative humidity. Separate experiments were performed to determine the effect of relative humidity on bond area. The increases in area over that at 50% RH were 2.0 and 4.2% at 75 and 90% RH, respectively. These changes would have negligible effect on the calculated values of the bond strength.

Table 6. Relative Humidity Dependence of Mean Bond Parameters.
(Lightly beaten, classified, unbleached pine kraft pulp)

Relative Humidity, %	Breaking Load, g	Bond Area, μm^2	Bond Strength, MPa
50	0.73	2100	3.5
75	0.60	2300	2.9
88	0.42	2200	2.1

Handsheets ($60\ g/m^2$) were also formed from these same (classified) fibers and were tested at 50, 75, and 92% RH. The strength results are presented in Table 7. The trends are similar to those for the individual fiber/fiber bonds. Changes in sheet properties are compared with those of fiber/fiber bond strength in Fig. 14. Here, the values of a particular parameter were normalized to the value for that parameter at 50% RH. Gurnagul and Page (33) have recently shown that there is little, if any, difference between the values of the zero-span test in the wet and dry states for unbleached, unbeaten pulps. Thus, the change in sheet values in

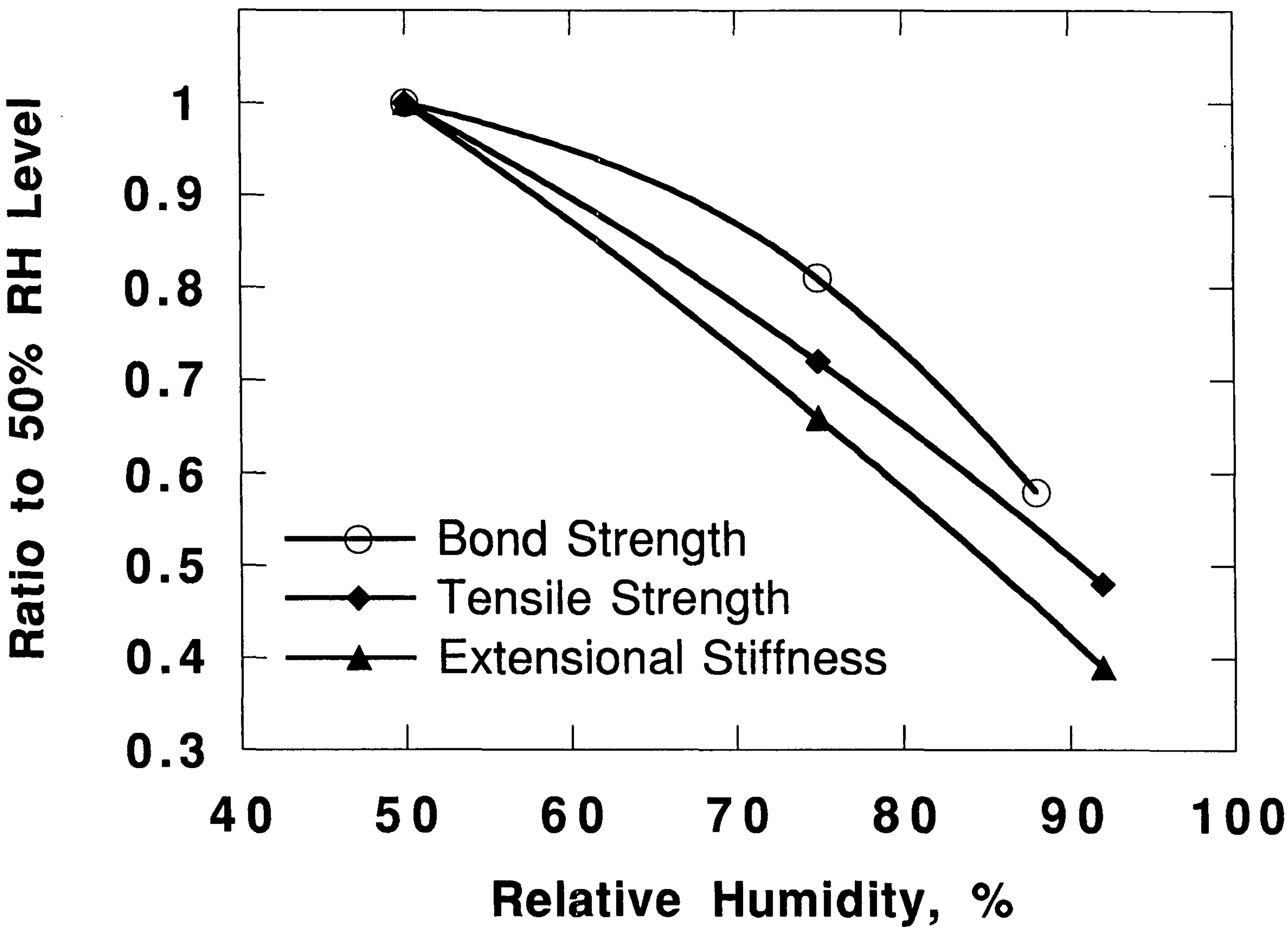

Fig. 14 Change of sheet and fiber properties with relative humidity normalized to the values at 50% RH.

Fig. 14 should mainly reflect changes in bond strength with increasing moisture content. The parallel behavior between sheet and fiber properties appears to bear this out.

Table 7. Effect of Relative Humidity on Sheet Properties.
(Lightly beaten, classified, unbleached pine kraft pulp)

	Relative Humidity, %		
	50	75	92
Moisture Content, %	5.0	10.5	15.5
Breaking Length, km	4.5	3.2	2.2
TEA, kgm/m^2	4.0	3.8	2.6
Et, kg/cm	350	230	140
Stretch, %	2.1	2.8	2.8
STFI, kN/m	1.26	0.77	0.58

FIBER WALL DAMAGE DURING BOND FAILURE

Degree of Damage

The SEM observations provided us a great deal of information concerning how and where bonds fail. Two extremes are shown in Figs. 15 and 16. The former was found most frequently with unrefined fibers untreated with strength aids, the latter with refined treated fibers. However, a variety of degrees of damage were found for a given pulp. For the fibers in Figs. 15 and 16, the degree of damage was 1 and 6, respectively. The damage type (see EXPERIMENTAL section for definition) for both these fibers was zero in contrast to those in Fig. 4 which was one.

Previous workers have presented microphotographs (optical, SEM, or TEM) of formerly bonded fibers. In some (8, 12) the magnification was too low to reveal much detail. In other studies (34-36),"picking" of microfibrils comparable to ranking 2 or 3 in Fig. 4 was found. Skowronski and Bichard (37) found different

Fig. 15 SEM of formerly-bonded fiber. Pulp: E0, Mount: BJ (T), TRank: 1, TType: 0.

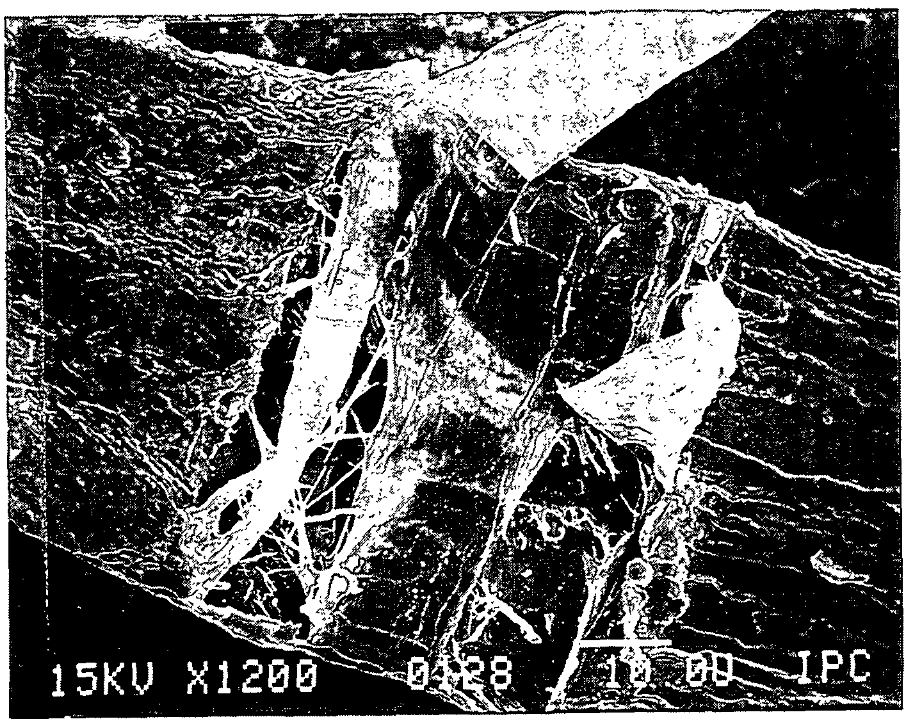

Fig. 16 SEM of formerly-bonded fiber. Pulp: EAC, Mount DV (T), TRank: 6, TType: 0.

types of bond failure when a delamination test was carried out at a slow strain rate compared with "impact" conditions. Although showing no examples, Thorpe et al. (16) described SEM results that showed fracture at the fiber/shive interface for a holocellulose (a ranking of 1 on our scale). For bonds formed from TMP at 110 or 210° C, they found failure within the fiber wall. In all of these studies, only single examples were given, and no systematic study of the relationship between bond strength and fiber damage was undertaken. The present study seeks to fill this gap.

The average values and standard deviations for the "rank" and "type" of damage for both axial (T) and cross (C) fibers for the several pulps are listed in Table 8. The damage values for the individual fibers are given in the Appendix.

Because the geometry of the loading experiment is nonsymmetrical (that is, the load is applied axially to one fiber and transversely to the other), it was of interest to determine the effect of this geometry on the damage produced during bond failure. The average damage ranking in the C (cross) direction for the 11 different pulps is plotted in Fig. 17 against the corresponding average ranking for the T (axial) fiber. The individual values are averages of about 40 fibers. The line drawn indicates identical values on each axis. There is no systematic dependence of damage on the experimental geometry.

There was, however, usually a wide variety of degrees of damage for a given pulp. The results for one pulp are shown in Fig. 18 where the rankings for the mates of individual fiber pairs have been summed. The severity of damage is seen to be normally distributed on this subjective ranking scale.

It would be expected that greater amounts of damage would be correlated with larger bond strengths, and there is some evidence that this is so. In Fig. 19 the logarithm of the average bond breaking load is plotted against the sum of the damage ratings of the mating fibers for the lightly beaten pulp (A5). Fiber pairs with like total damage values were grouped together, and their average breaking load and its standard error are shown. The line shown is a least squares fit to the data. Greater damage is associated with stronger bonds.

Table 8. Mean Fiber Bond Damage Properties.

Fiber	Code	Additives [a]	R.H., %	CRank	TRank	CType	TType
Earlywood	E0	--	50	2.08 (0.50)[b]	2.00 (0.45)	0.00 (0.00)	0.00 (0.00)
Latewood	L0	--	50	2.46 (0.88)	2.50 (0.78)	0.00 (0.00)	0.00 (0.00)
Earlywood	EAC	A/C	50	3.67 (1.04)	3.62 (1.59)	0.00 (0.00)	0.00 (0.00)
570 mL CSF	A5	--	50	3.82 (0.96)	3.40 (1.04)	0.82 (0.38)	0.81 (0.40)
570 mL CSF	A75	--	75	3.90 (1.23)	3.71 (1.02)	0.74 (0.44)	0.69 (0.47)
570 mL CSF	A88	--	88	3.80 (1.14)	3.41 (0.86)	0.71 (0.46)	0.73 (0.45)
570 mL CSF	AAC	A/C	50	4.34 (1.15)	4.38 (1.17)	0.58 (0.50)	0.66 (0.48)
570 mL CSF	ADS	D/S	50	4.07 (1.01)	4.67 (0.87)	0.77 (0.43)	0.70 (0.47)
345 mL CSF	A3	--	50	4.41 (0.91)	3.98 (0.80)	0.92 (0.27)	0.81 (0.39)
TMP	T0	--	50	3.15 (0.84)	3.04 (0.71)	0.51 (0.51)	0.80 (0.41)
TMP	TAC	A/C	50	4.32 (1.07)	4.25 (0.98)	0.73 (0.45)	0.79 (0.41)

a) Fibers treated with A/C (see text) or D/S polymers.

b) Values in parentheses are standard deviations.

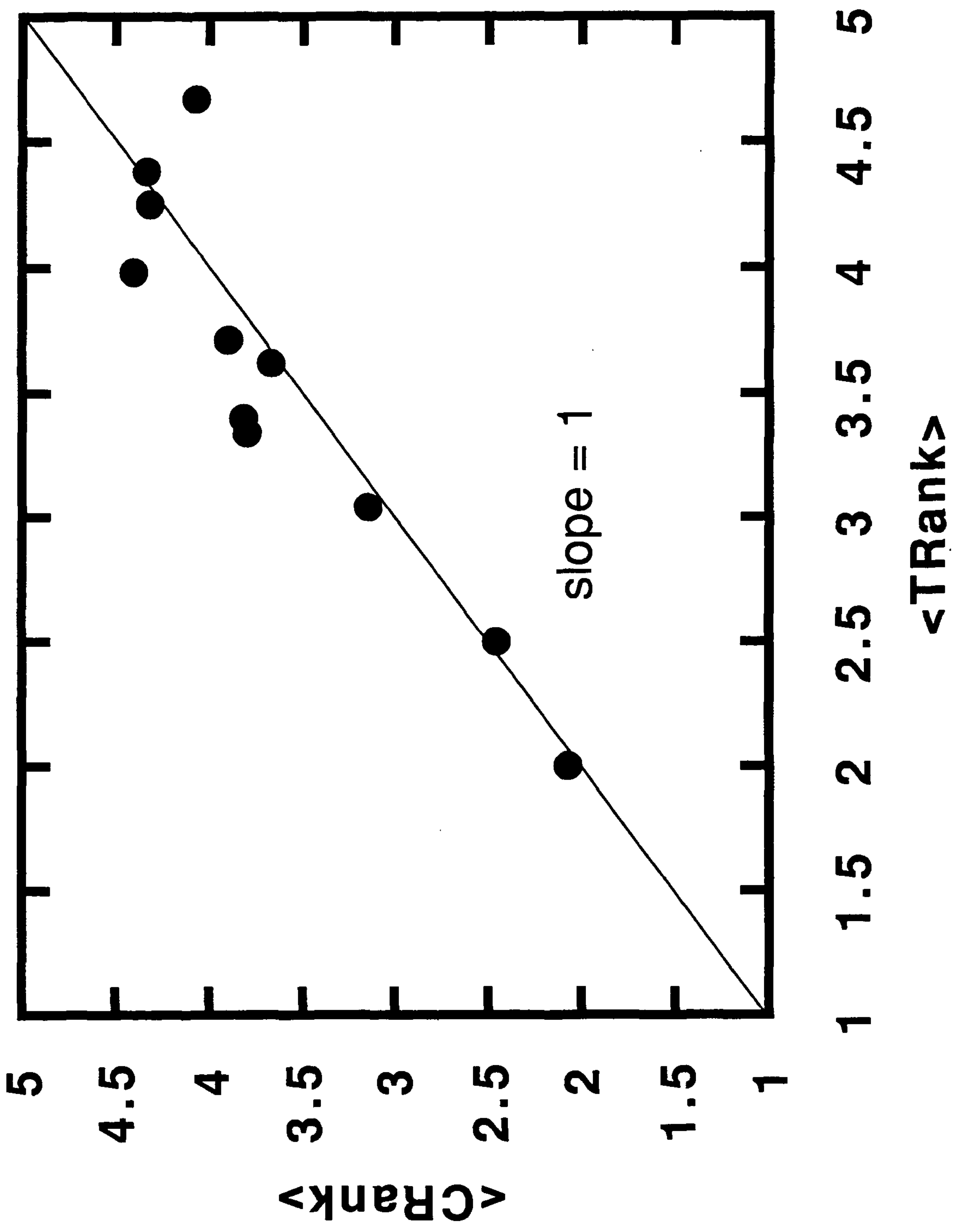

Fig. 17 Independence of damage rating on fracture geometry.

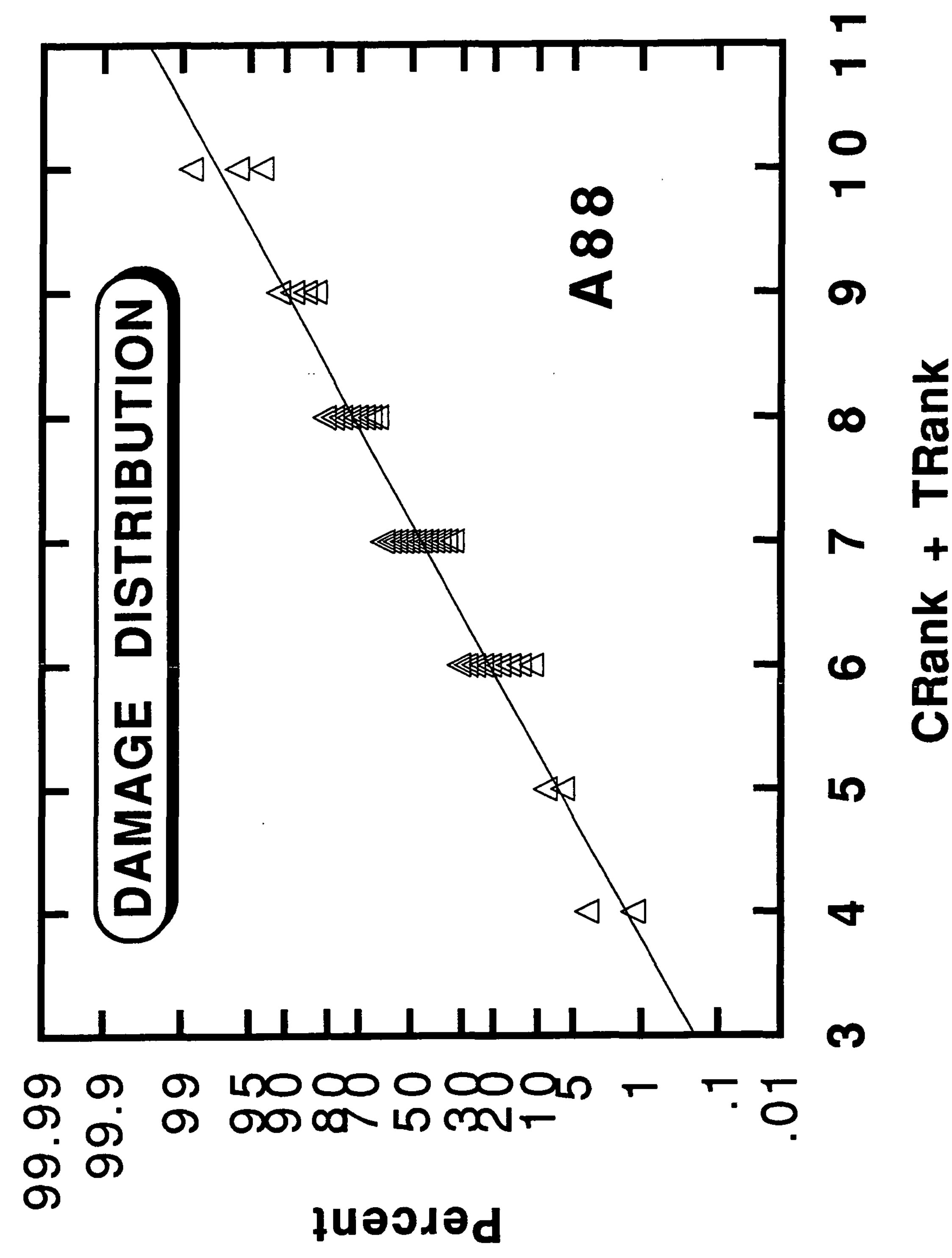

Fig. 18 Normal probability distribution of damage rating for the population of bonds formed from pulp A88.

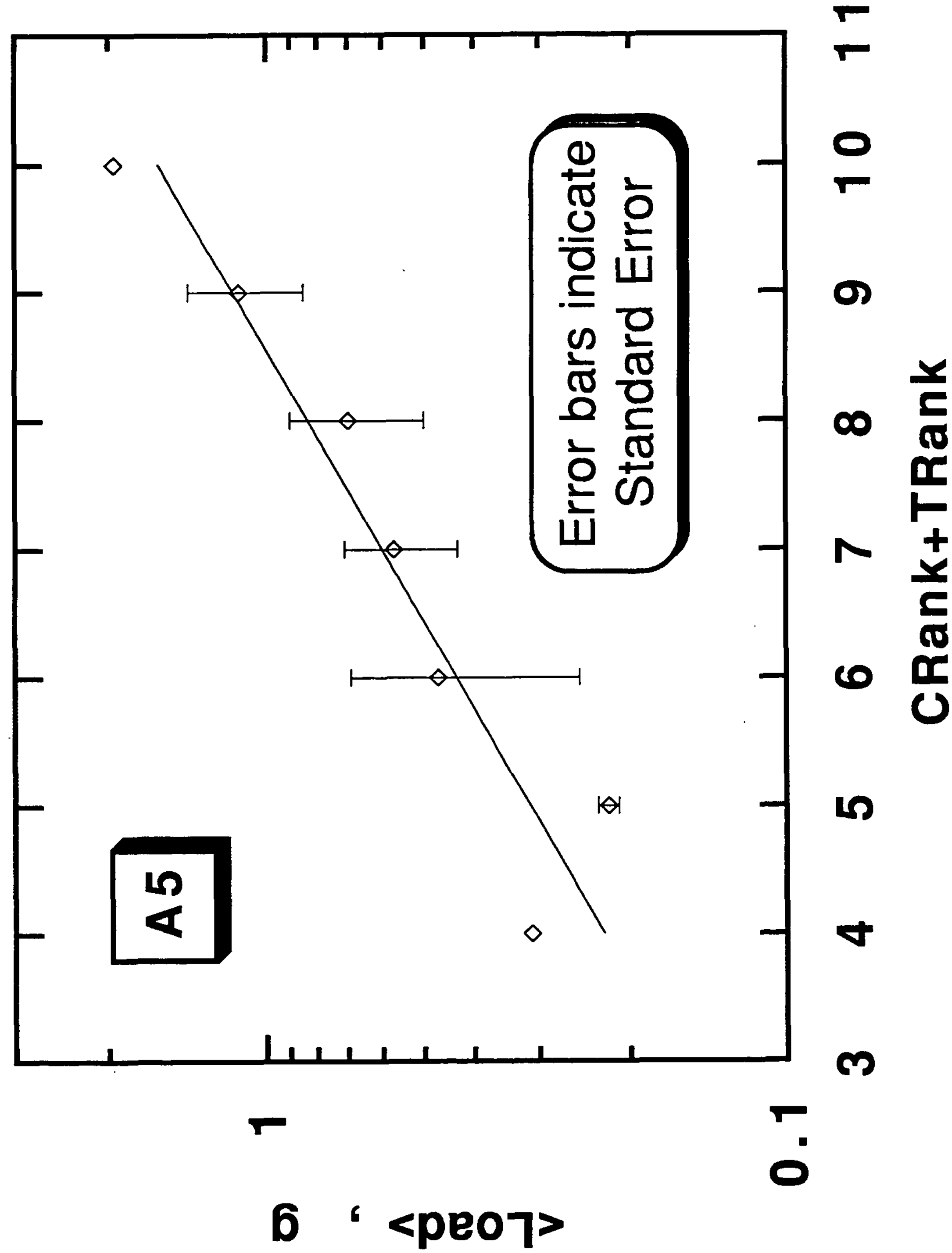

Fig. 19 Correlation of average bond breaking load with damage rating for pulp A5.

An alternative presentation can be made in terms of the bond strength. Again, values at the same damage ranking were grouped and averaged. The results are shown in Fig. 20.

For comparison, the bond strength values for the same pulp treated with the "ionic only" strength aid (ADS) are given. The error bars indicate the standard error of the bond strength at each ranking, and the lines drawn are least squares fits to the data. The tips of the arrows indicate the overall average bond strength and damage ranking for each pulp. Obviously, the strength aid increases both the bond strength and the severity of damage to the fibers.

This is apparently a general result as shown by the values in Table 9. For three different pulps, the presence of either A/C or D/S produces greater damage when the fiber/fiber bond is ruptured. For the earlywood pulp, the locus of failure is shifted from the interface between the fibers to within the fiber wall. Addition of A/C to this pulp reduces the amount of rank 1 damage (i.e., no damage, see Fig. 4) from about 10% to less than 2% of the samples. Since the amount of strength aid added is equivalent to less than a monolayer of the polymer (25), there is no continuous "film" of adhesive between the two fibers. Instead, the strength aid is providing additional individual bonds within the bonded area.

Table 9. Effect of Strength Aids on Fiber Damage.

Pulp	CRank + TRank	
	Untreated	Treated
Earlywood	4.1	7.3
TMP	6.2	8.6
A5	7.2	8.7(A/C), 8.7(D/S)

Examining the results in Table 8, we find that relative humidity has no statistically significant effect on the amount of damage occurring during bond failure. There is a small increase in the amount of damage when the A5 pulp (570

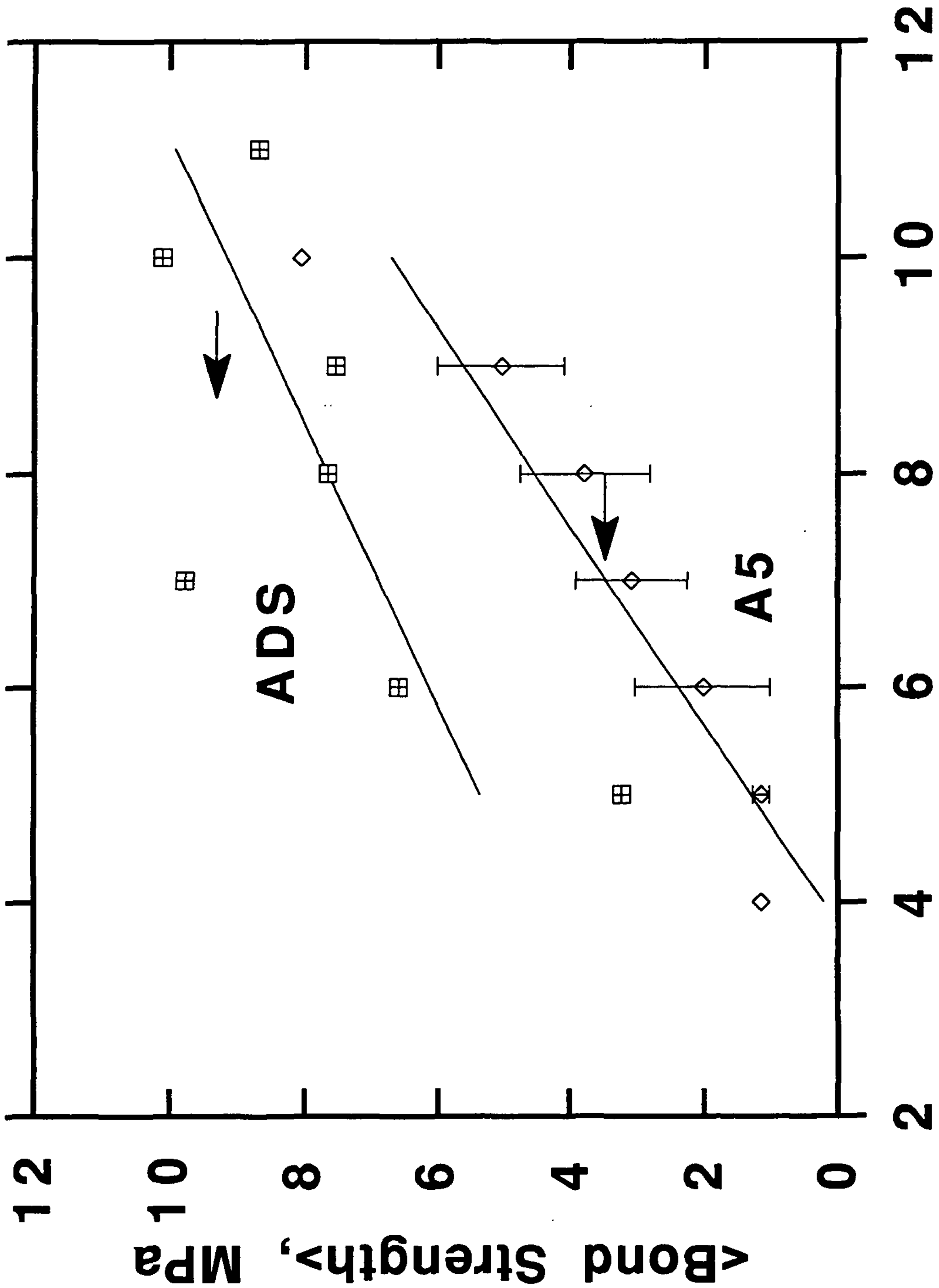

Fig. 20 Effect of strength aid on damage rating for the lightly refined pulp. Tips of arrows indicate overall average values for strength and damage rating for each pulp.

mL CSF) is further refined to the A3 (345 mL CSF) conditon. However, it is not possible to differentiate between the additional damage produced by the refining operation from that which might be caused by the more intimate contact available to the A3 fibers.

Finally, we can say with greater than 99% certainty that more damage occurs when the bond between two latewood fibers fails than the corresponding case for two earlywood fibers. This result parallels the greater strength of the latewood bond noted above.

Evidence for the "Skirt" Effect

As mentioned above, some of the formerly-bonded fibers possessed additional fibrillated or wall material along their edges. As it happens, all of the fibers chosen as archetypes for the damage ranking (Fig. 4) were of this type, while those shown in Figs. 15 and 16 were not. The two types were assigned ratings of 0 (material absent) or 1 (material present) without regard for the amount of material. At the time we were puzzled by these fragments whose presence seemed independent of the amount of damage in the central regions of the bond. We now believe that they are a result of and further evidence for the "skirt" effect recently discovered by Nanko and Ohsawa (38). This phenomenon is shown in Fig. 21 taken from their paper. The skirt is formed by the adhesion of the S1 layer, which has swollen and separated from the S2 layer of the same fiber, to the surface of the mating fiber. Nanko and Ohsawa found this separation in both refined and unrefined fibers and suggested it occurred in the latter as a result of the pressing operation. We only found type 1 behavior for refined pulps. Significantly, we did not find it for unrefined, earlywood fibers treated with a strength aid which showed large amounts of damage in the central regions of the bonds. Apparently, for this pulp, S1-S2 separation did not occur during bond formation. The different species of pulp, Japanese beech and loblolly pine, may account for the presence or absence of S1-S2 separation for unrefined pulp.

Additional evidence for the skirt effect is adduced in Fig. 22-24. The fibers in Figs. 22 and 23 were mates from a single bond, and both show the effect. Considerable tearing (peeling) of S1 material is also exhibited in Fig. 23. Such tearing was most commonly found when strength aids were used (cf. Fig. 16) but

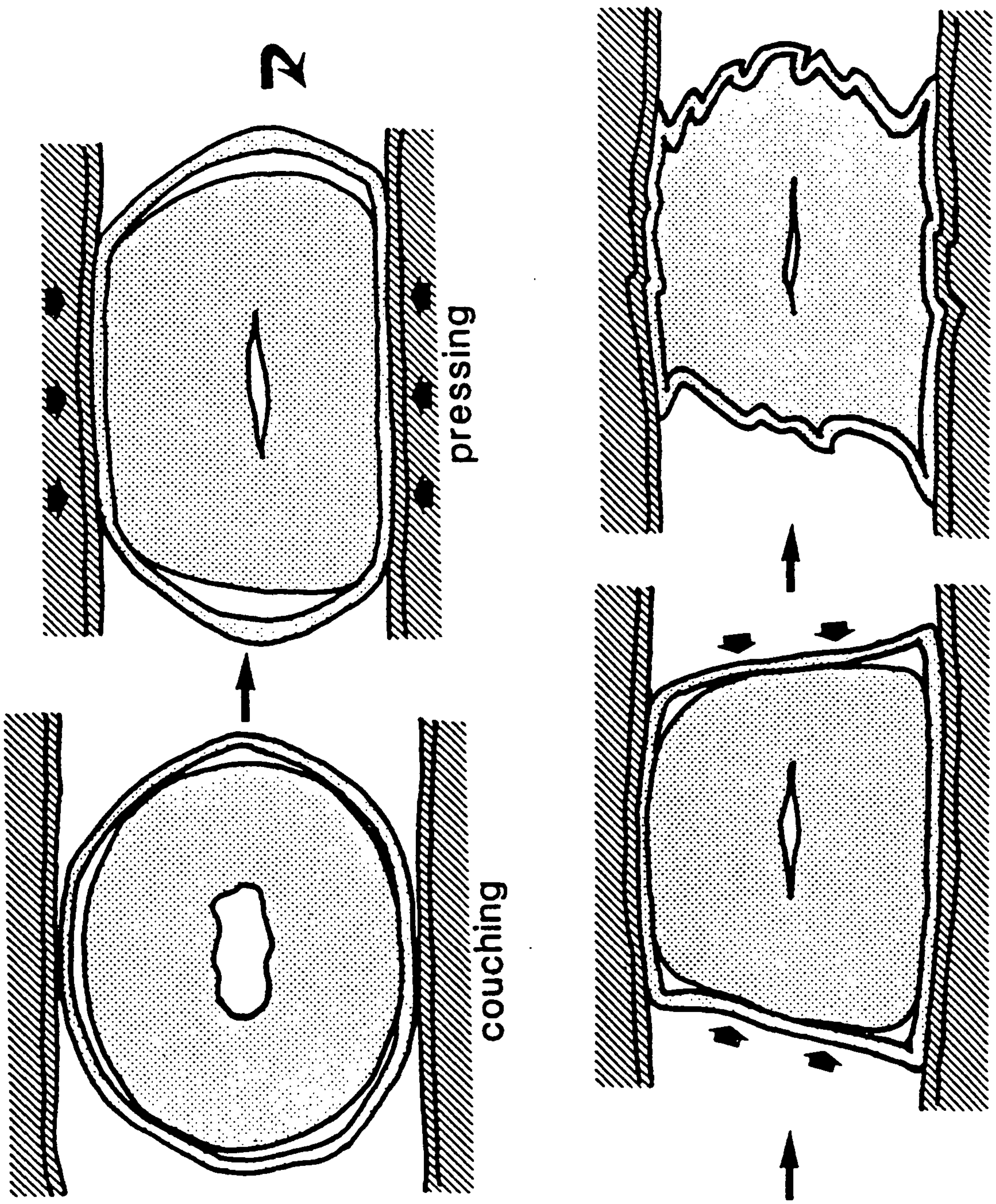

Fig. 21 Schematic representation of the changes occurring during fiber bond formation. Taken from Nanko and Ohsawa (38).

Fig. 22 SEM of formerly-bonded fiber showing skirt material. Pulp: A5, Mount: JK (T).

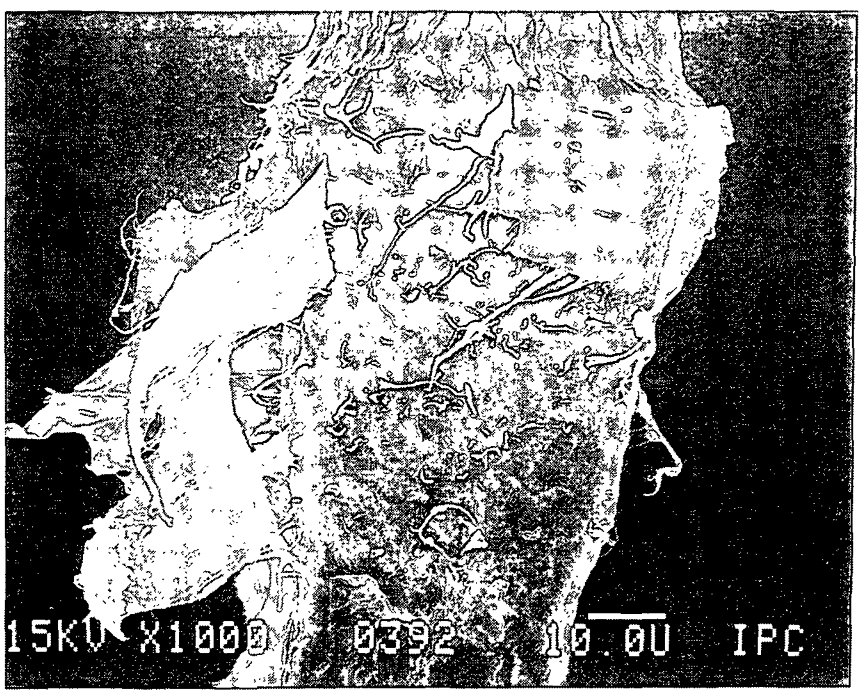

Fig. 23 SEM of formerly-bonded fiber showing skirt material. Pulp: A5, Mount: JK (C) (Mate to fiber in Fig. 22).

was also observed for other well-bonded samples. Apparently, the bond strength between the mating S1 layers of the two fibers is greater than that between the S1 and S2 layers of one or the other of the fibers.

The rupture of the skirt material is perhaps most clearly shown in Fig. 24. Here, the peeled-back skirt material and its locus of fracture are obvious. The locus is shown schematically in Fig. 25 which can be viewed as a close-up of the interface region of the dried state in the Nanko and Ohsawa schematic (Fig. 21). They suggest that the presence of the skirts is important for increasing the strength of fiber/fiber bonds. More important than the additional bond area that the skirts provide is their role in distributing the stress at the periphery of the bond. The stress concentrations that are expected to be large here are reduced and redistributed by the skirts, and a higher load can be sustained. As the applied load is increased further, stress concentrations eventually lead to bond failure. The evidence from our SEM photos suggests the locus of failure of the S1 layer to be in the vicinity of the arrow drawn in Fig. 25; that is, the peak stress is not at the outer edge of the bond but is slightly inside it. To improve bond strength further would require strengthening the material in the S1 layer.

The reduction of stress concentration by the skirt material is supported by our strength data. Bond strength is plotted in Fig. 26 against the rating for the evidence of this skirt material on the mating fibers. Thus, values of 0, 2, or 1 on the abscissa indicate that neither, both, or only one of the fibers showed this material. For both the untreated (A5) and treated (ADS) pulps, the trend is clear: bond strength increases when the skirt material is present. The error bars show the standard error, while the tips of the arrows indicate the overall average values for the bond strength and (CType + TType) value. Note that the average value for this latter parameter is approximately the same for both pulps even though the strength aid increases the bond strength substantially. Apparently, the skirt effect is little influenced by additives.

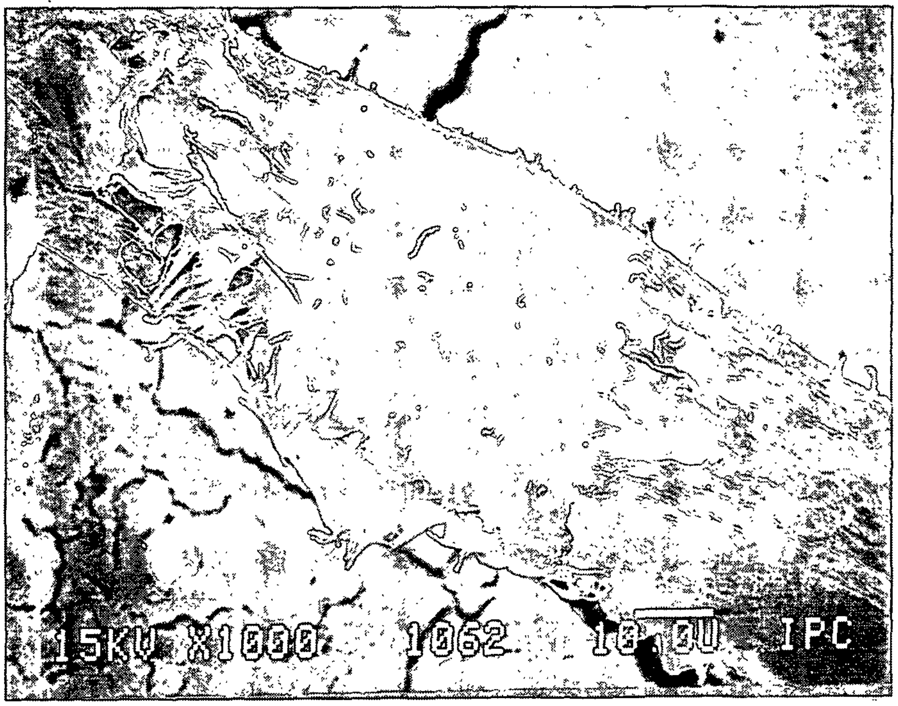

Fig. 24 SEM of formerly-bonded fiber showing fracture zone of skirt material. Pulp: A75, Mount: XU (T).

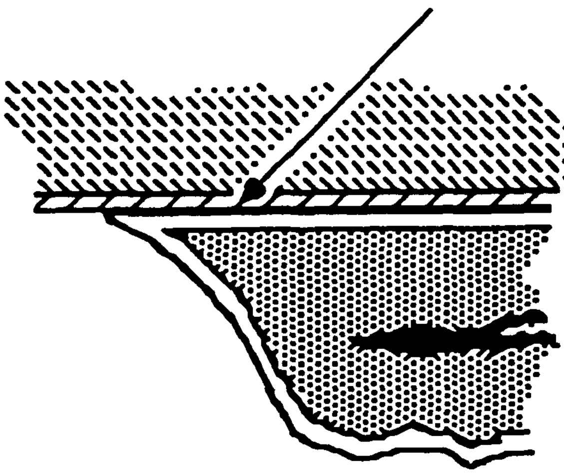

Fig. 25 Schematic representation of the location of fracture of the S1 layer.

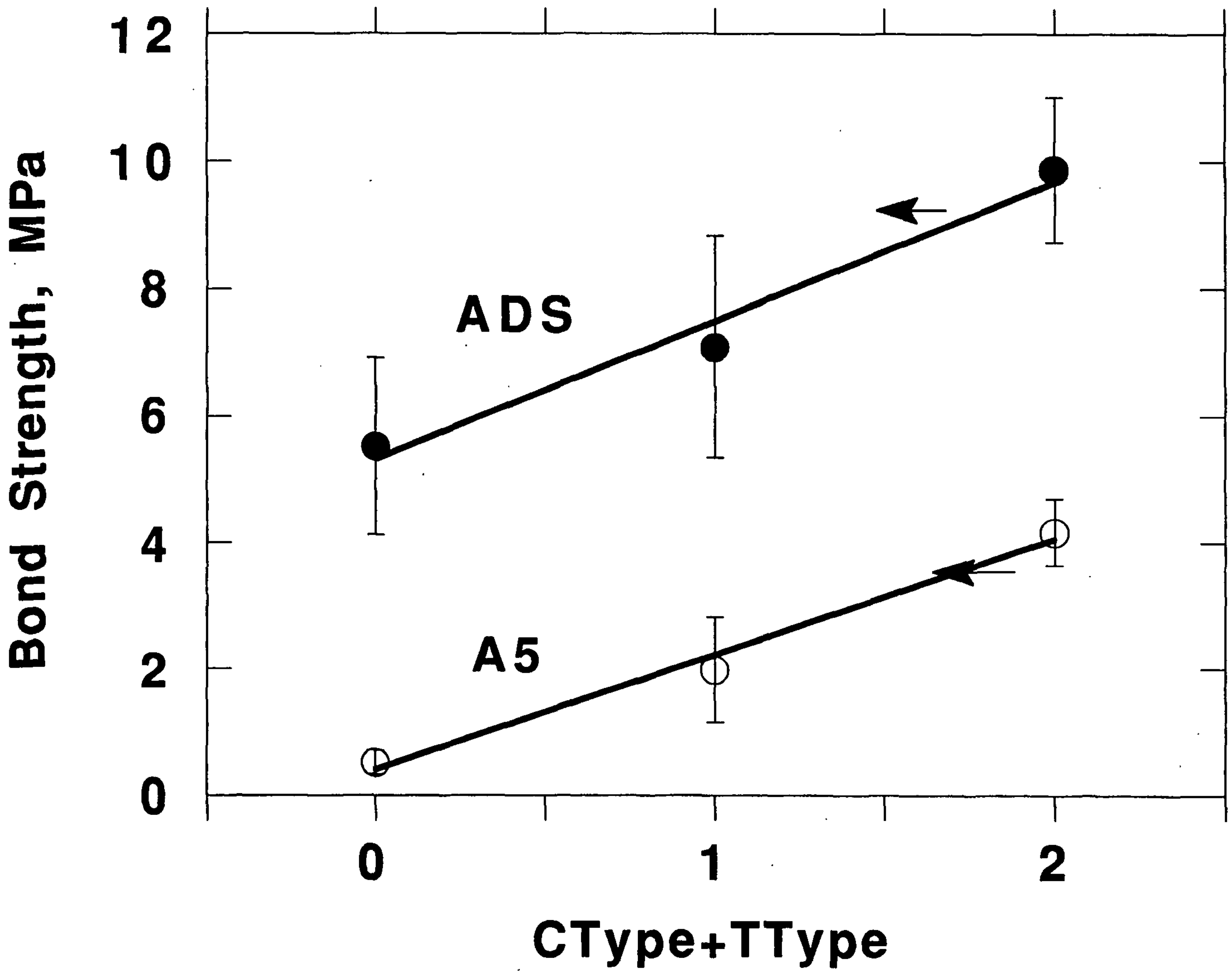

Fig. 26 Dependence of bond strength on the presence of "skirt" material. Tips of arrows indicate overall average values for strength and amount of skirt material for each pulp.

SUMMARY

The bond strength of individual fiber/fiber bonds has been determined using new instrumentation. In agreement with some previous workers, we find that bonds formed with latewood fibers are stronger than those from earlywood fibers and that refining has a negligible effect on bond strength. In contrast to previous work, we find that polymeric strength aids can enhance the bond strength by a factor of two. Increasing the relative humidity (moisture content) decreases the bond strength in parallel to the loss of sheet strength.

Scanning electron micrographs revealed that the degree of damage to the fiber wall during bond fracture correlated with bond strength. With larger values of the latter, there was a shift of locus of fracture from between the two fibers to within the fiber walls. It was noted that for some of the ruptured bonds significant amounts of torn S1 material was located along the edge of the fiber in the region of the former bond. We interpreted this to be evidence of "skirt" material. A positive correlation between the presence of this material and the magnitude of the bond strength suggested that the skirt functions to reduce the stress concentration in the periphery of the bond area.

ACKNOWLEDGEMENTS

The authors are indebted to Mr. Keith W. Hardacker for advice and help in measuring the bond breaking load. Mr. Norman L. Colson carried out all phases of the experimental work reported here. His innovation in the development of techniques for the preparation and handling of the single fiber bonds was crucial to the successful completion of this project. His conscientious efforts and attention to detail have resulted in a reliable body of data comprising hundreds of fiber/fiber bonds and are greatly appreciated. The expertise and patience of Mrs. Mary Block and Ms. Ellen Foxglover in obtaining the SEM photographs is gratefully acknowledged.

LITERATURE CITED

1. Becher, J. J., Stratton, R. A., and Baum, G. A., Fundamentals of Internal Strength Enhancement, Part One: Improved Bonding via Chemical Additives, Project 3526, Report One, The Institute of Paper Chemistry, Appleton, WI, September 15, 1984.

2. Becher, J. J., Stratton, R. A., and Baum, G. A., Fundamentals of Internal Strength Enhancement, Part One: Improved Bonding via Chemical Additives, Project 3526, Report Two, The Institute of Paper Chemistry, Appleton, WI, September 30, 1986.

3. Page, D. H., Tappi 52, 674 (1969).

4. Kallmes, O., and Perez, M., in Consolidation of the Paper Web, edited by F. Bolam, Tech. Sec. Brit. Paper and Board Makers Assoc., London, (1966), p. 779.

5. Van den Akker, J. A., Lathrop, A. L., Voelker, M. H., and Dearth, L. R., Tappi 41, 416 (1958).

6. Page, D. H., El-Hosseiny, F., Winkler, K., and Bain, R., Pulp Paper Mag. Can. 73, T198 (1972).

7. Hardacker, K. W., and Brezinski, J. P., Tappi 56 (4), 154 (1973).

8. Mayhood, C. H., Kallmes, O. J., and Cauley, M. M., Tappi 45 (1), 69 (1962).

9. McIntosh, D. C., Tappi 46, 273 (1963).

10. Schniewind, A. P., Nemeth, L. J., and Brink, D. L., Tappi 47, 244 (1964).

11. Russell, J., Kallmes, O. J., and Mayhood, C. H., Tappi 47 (1), 22 (1964).

12. Mohlin, U.-B., Svessk Papperstidn. 77 (4), 131 (1974).

13. Hartler, N., and Mohlin, U.-B., Svensk Papperstidn. 78 (8), 295 (1975).

14. Mohlin, U.-B., Svensk Papperstidn. 78 (9), 338 (1975).

15. Mohlin, U.-B., Svensk Papperstidn. 78 , 373 (1975).

16. Thorpe, J. L., Mark, R. E., Eusufzai, A. R. K., and Perkins, R. W., Tappi 59 (5), 96 (1976).

17. Button, A. F., Doctoral Dissertation, The Institute of Paper Chemistry, Appleton, WI., 1979.

18. Page, D. H., Paper Tech. 1, 407 (1960).

19. Page, D. H., and Tydeman, P. A., Paper Tech. 1, 519 (1960).

20. Page, D. H., Tydeman, P. A., and Hunt, M., in Formation and Structure of Paper, edited by F. Bolam, Tech Sec. Brit. Paper and Board Makers Assoc., London, 1962, p. 171.

21. Uesaka, T., in Handbook of Physical and Mechanical Testing of Paper and Paperboard, (R. E. Mark, ed.), Vol. 2, Marcel Dekker, New York, (1984), p. 379.

22. Brezinski, J. P., and Hardacker, K. W., Unpublished work, The Institute of Paper Chemistry, Appleton, WI, 1972.

23. Wink, W. A., Unpublished work, The Institute of Paper Chemistry, Appleton, WI, 1980.

24. Espy, H. H., Proc. 1983 TAPPI Papermakers' Conf., TAPPI Press, Atlanta, p. 191.

25. Stratton, R. A., Nordic Pulp Paper Res. J. 4, 104 (1989).

26. Espy, H. H., and Rave, T. W., Tappi J. 71 (5), 133 (1988).

27. Becher, J. J., and Stratton, R. A., Unpublished work, The Institute of Paper Chemistry, Appleton, WI, 1984.

28. Hardacker, K. W., Tappi 45, 237 (1962).

29. Hardacker, K. W., Unpublished work, The Institute of Paper Chemistry, Appleton, WI, 1985.

30. Nordman, L. S., and Qvickstrom, B., in The Physics and Chemistry of Wood Pulp Fibers, edited by D. H. Page, TAPPI Press, New York, 1970, p. 177.

31. Ingmanson, W. L., and Thode, E. F., Tappi 42 (1), 83 (1959).

32. Stratton, R. A., Proc. 1991 International Paper Physics Conference, Kona, HI, p. 561.

33. Gurnagul, N., and Page, D. H., Tappi J. 72 (12), 164 (1989).

34. Jayme, G., and Hunger, G., in Formation and Structure of Paper, edited by F. Bolam, Tech Sec. Brit. Paper and Board Makers Assoc., London, 1962, p. 135.

35. Page, D. H., and Sargent, J. W., in Formation and Structure of Paper, edited by F. Bolam, Tech Sec. Brit. Paper and Board Makers Assoc., London, 1962, p. 201.

36. Buchanan, J. G., and Lindsay, R. A., in Formation and Structure of Paper, edited by F. Bolam, Tech Sec. Brit. Paper and Board Makers Assoc., London, 1962, p. 101.

37. Skowronski, J., and Bichard, W., J. Pulp Paper Sci. 13 (5), J165 (1987).

38. Nanko, H., and Ohsawa, J., in Fundamentals of Papermaking, edited by C. F. Baker, Mechanical Engineering Publications Ltd., London, 1989, p.783.

Robert A. Stratton
Associate Professor
Senior Research Scientist
Institute of Paper Science and Technology

APPENDIX

FIBER/FIBER BOND PROPERITES

Earlywood Data (E0)

Mount	Load (g)	Area (μm^2)	BondStr (MPa)	CRank	TRank	CType	TType
AU	0.330	2050	1.58			0	0
AV	0.069	2226	0.30		2	0	0
AX	0.588	2408	2.39	2	2	0	0
AY	0.533	1157	4.51	2	2	0	0
BA	0.989	2698	3.60	2	2	0	0
BB	0.088	2579	0.33	2	1	0	0
BC	0.231	2310	0.98	2	2	0	0
BD	0.137	2480	0.54	2	2	0	0
BE	0.615	2700	2.23	2	3	0	0
BG	0.159	1133	1.37	3	2	0	0
BH	0.626	2013	3.05	3	3	0	0
BI	0.560	2447	2.83	2	3	0	0
BJ	0.176	1787	0.97	1	1	0	0
BK		3888					
BL	0.648	601.0	10.57	2	2	0	0
BM	1.280	2194	5.72	2	2	0	0
BN	0.165	673.0	2.40	2	2	0	0
BO	1.082	3274	3.24	2	2	0	0
BP	0.291	2902	0.98				
BQ	0.319	1520	2.06	2	2	0	0
BR	0.099	1826	0.53	2	2	0	0
BS	0.104	3055	0.33	2	2	0	0
BT	0.676	1289	0.90				
BU	0.643	3446	1.83		2		0
BV	0.813	2640	3.02	2	2	0	0
BW	0.451	2028	2.18	2	3	0	0
BX	0.412	2497	1.62	2	2	0	0
BY	0.165	3132	0.52	2		0	
BZ	0.198	1908	1.02	2	2	0	0
CA	0.231	3455	0.66	2	2	0	0
CB	0.956	2759	3.40	3	2	0	0
CC	0.154	2887	0.52	3	2	0	0
CD	0.313	1563	1.96		1		0
CE	0.286	2634	1.06		2		0
CF		3139			2		0
CG	0.143	2339	0.60	2	2	0	0

Earlywood Data (E0) (Continued)

Mount	Load (g)	Area (μm^2)	BondStr (MPa)	CRank	TRank	CType	TType
CH		3268					
CI	0.187	2067	0.89	2	2	0	0
CJ	0.236	3335	0.69	2	2	0	0
CK	0.231	2099	1.08	2	2	0	0
CL		2402					
CM	0.225	1588	1.39	3	2	0	0
CN	0.258	4084	0.62	3	2	0	0
CO	0.945	2529	3.67		2		0
CP	0.725	1211	5.87	2	2	0	0
CQ	0.104	1522	0.67	1	1	0	0
CR	2.843	4309	6.47				
CS	0.181	3482	0.51	1	2	0	0

Earlywood (Treated with A/C) Data (EAC)

Mount	Load (g)	Area (μm^2)	BondStr (MPa)	CRank	CType	TRank	TType
CT	1.52	3000	4.37	4	0	3	0
CU	0.90	2320	3.79	4	0	4	0
CV	2.79	4058	6.73	3	0	6	0
CW	0.62	2328	2.61			2	0
CX	0.61	3654	1.63				
CY	0.83	2297	3.53	2	0	5	0
CZ	1.68			5	0	6	0
DA	0.79	2042	3.78	3	0	3	0
DB		3097					
DC	1.51	1916	7.70	3	0	2	0
DD	1.47	3000	4.45				
DE	0.95	2621	3.57	3	0	6	0
DF	1.35	4025	3.28	3	0	2	0
DG	1.41	2642	5.24				
DH	1.52	3389	4.39	4	0	3	0
DI	1.30	3108	4.11	5	0	5	0
DJ	1.01	4137	2.39			6	0
DK	0.61	4255	1.41	3	0	4	0
DL	0.82	3967	2.02				
DM		2617					
DN		2254					
DO	0.94	4882	2.00	4	0	4	0
DP	0.77	3381	2.23				
DQ	0.70	2253	3.05	4	0	6	0
DR	0.77	2109	3.58	3	0	3	0
DS	0.71	2874	2.43	3	0	2	0
DT		3406					
DU	1.32	1946	6.66				
DV	1.68	2708	6.09			6	0
DW	1.12	3685	2.97	3	0	2	0
DX	1.95	3003	6.36	3	0		
DY	1.23	3361	3.59	4	0	3	0
DZ	0.57	1687	3.31	3	0	2	0
EA	0.57	1827	3.08	4	0	5	0
EB	1.46	2587	5.53	6	0	2	0
EC	1.26	3005	4.12	6	0	1	0
ED	0.60	3040	1.93	4	0	4	0
EE	1.69	2706	6.12	5	0	2	0
EF	0.68	3645	1.84	2	0	3	0
EG	1.28	2511	5.00	3	0	3	0

Latewood Data (L0)

Mount	Load (g)	Area (μm^2)	BondStr (MPa)	CRank	CType	TRank	TType
Ll	1.04	1533	6.66	2	0	2	0
Lm	1.75	1306	13.13	1	0	2	0
Ln	0.92	1192	7.55	2	0	2	0
Lo	0.74	891	8.12	2	0	2	0
Lp	1.19	1217	9.57	2	0	2	0
Lr	2.05	1653	12.16	2	0	3	0
Ls	0.91	1209	7.40	2	0	2	0
Lt	1.61	2126	7.43	2	0	2	0
Lu	0.31	1015	2.95	3	0	3	0
Lv	0.18	1899	0.91	3	0	3	0
Lw	0.41	1966	2.05	1	0	3	0
Lx	0.24	2155	1.11			1	0
Ly	2.06	2132	9.47	2	0	3	0
Lz	0.21	2188	0.92	2	0	1	0
Mb	0.51	1433	3.49	3	0	2	0
Mc	1.31	1318	9.77	2	0	3	0
Md	0.27	2249	1.16	2	0	2	0
Me	0.77	675	11.13	2	0	2	0
Mf	0.44	532	8.18	3	0	3	0
Mg	1.77	1907	9.08	3	0	2	0
Mi	0.70	1645	4.17	3	0	2	0
Mj	1.58	1238	12.50	3	0	3	0
Mk	0.45	1213	3.66	3	0	4	0
Ml	1.59	1267	12.29	2	0	2	0
Mm	0.59	1554	3.70	2	0	4	0
Mo	0.40	856	4.58	3	0	2	0
Mp	0.99	1712	5.69	2	0	2	0
Mq	0.38	3450	1.07	2	0	3	0
Mu	0.61	2114	2.83	3	0	4	0
Mv	0.62	1394	4.34	2	0	2	0
Mw	1.53	950	15.77	2	0	2	0
My	0.27	1093	2.39	6	0	4	0
Mz	1.03	792	12.69	3	0	3	0
Nao	1.15	1397	8.05	4	0	4	0
Nb	0.58	1743	3.25	3	0	2	0
Nc	0.65	1275	5.02	2	0	2	0
Nd	1.76	1584	10.88	4	0	3	0
Ne	0.66	1172	5.53	2	0	2	0
Nf	0.29	1322	2.18	2	0	2	0
Ng	0.18	1528	1.15	2	0	3	0

Unbleached Kraft Pulp (570 mL CSF) Data (A5)

Mount	Load (g)	Area (μm^2)	BondStr (MPa)	CRank	CType	TRank	TType
HT	0.23	3525	0.65	3	1	4	1
HU	1.49	2816	5.17	5	1	4	1
HV	0.39	1770	2.18	4	1	5	1
HW	1.86	1731	10.54	3	1	4	1
HX	0.19	1207	1.55	4	1	3	1
HY	2.83	2906	9.56	5	1	4	1
HZ	0.79	1284	6.06	4	1		
IA		2938					
IB	0.66	1447	4.48	5	1	4	1
IC	0.52	2404	2.12	3	0	4	1
ID	0.19	1792	1.05	2	0	3	1
IE	0.56	1254	4.39	4	1	3	1
IF	0.17	1846	0.92	4	1	4	0
IH	0.22	2550	0.83	3	1	2	1
II	0.19	3632	0.51	4	0	3	1
IJ	0.31	2644	1.15	2	1	2	1
IK	0.58	2501	2.28	3	0	3	1
IL	1.95	2373	8.06	5	1	5	1
IM	0.86	2281	3.71	5	1	3	1
IN	0.69	1537	4.37	4	1	3	1
IO	0.58	2686	2.13	4	1	3	1
IP	0.20	1582	1.24			2	1
IQ	0.25	1757	1.38	2	1	3	1
IR		1395					
IS	0.41	1675	2.39	3	1	5	1
IT	1.21	1318	8.97	4	1	4	1
IU	0.79	1766	4.39	4	1	5	1
IV	1.49	2917	5.01	4	1	4	1
IW	0.16	961	1.59	4	1	5	1
IX	1.00	1753	5.61	3	1	4	1
IY	0.06	1848	0.31	5	1	2	0
IZ	0.89	3568	2.45			1	0
JA	0.19	2103	0.89	5	0	4	1
JB	1.04	2142	4.75	2	1	4	1
JC	0.53	2523	2.07	3	1	4	1
JD		1601					

Unbleached Kraft Pulp (570 mL CSF) Data (A5) (Continued)

Mount	Load (g)	Area μm^2)	BondStr (MPa)	CRank	CType	TRank	TType
JE	0.22	1583	1.34	3	1	2	0
JF	1.86	2133	8.53	5	1	4	1
JG	0.40	1434	2.71	4	1	3	1
JH	1.51	3324	4.46			1	0
JI	0.07	269	2.69	4	1	4	1
JJ	0.16	2214	0.70	3	0	3	0
JK	0.67	2300	2.85	5	1	3	1
JL	2.00	2303	8.51	5	1	4	0
JM		1404					
JN	0.91	1715	5.20	5	1	4	1
JO	0.09	2652	0.33	4	0	2	0

Unbleached Kraft Pulp (Treated with A/C) Data (AAC)

Mount	Load (g)	Area (μm^2)	BondStr (MPa)	CRank	CType	TRank	TType
Jp	0.74	1379	5.25	3	1	3	1
Jq	0.63	1421	4.33	6	1	5	1
Jr	1.92	1514	12.40	3	1	4	1
Js	1.46	1866	7.66	6	0	5	1
Jt	0.72	3402	2.08	5	0	4	0
Ju	1.62	1781	8.90	5	0	6	0
Jv	0.54	2005	2.64	3	1	5	1
Jw	0.51	1950	2.58	4	0	3	0
Jx	0.87	2270	3.74	5	1	5	1
Jy	0.41	1850	2.18	3	0	3	0
Jz	0.21	1414	1.48	2	1	4	1
Ka	1.13	2118	5.24	2	1	3	1
Kb	0.74	2205	3.28	4	0	5	1
Kc	1.67	1498	10.94	4	1	5	1
Kd	1.52	2140	6.94	1	0	4	1
Ke	3.40	1330	25.08	4	1	4	1
Kf	2.01	2425	8.13	5	1	4	1
Kg	1.79	2072	8.45	5	0	5	1
Kh	0.93	3636	2.51	5	0	4	1
Ki	0.40	1624	2.41	4	0	5	0
Kj	2.01	3473	5.68	4	0	5	0
Kk	0.71	1474	4.73	4	0	5	1
Kl	0.52	1766	2.90	4	0	5	0
Km	1.16	2550	4.46	5	1	2	0
Kn	1.02	2637	3.80	4	1	5	0
Ko	1.29	1464	8.66	5	1	6	1
Kp	3.06	2141	13.99	5	1	6	1
Kq	0.58	1887	3.01	5	0	3	1
Kr	1.97	1242	15.56	5	1	5	1
Ks	0.93	1116	8.20	4	1	3	1
Kt	0.52	1265	4.04	5	0	5	1
Ku	1.02	1615	6.19	4	0	5	1
Kv	2.31	2463	9.18	5	1	2	1
Kw	6.72	2572	25.62	4	1	4	1
Kx	0.58	2596	2.19	4	1	6	0
Ky	0.89	1901	4.58	6	1	6	0

Unbleached Kraft Pulp (Treated with A/C) Data (AAC) (Continued)

Mount	Load (g)	Area (μm^2)	BondStr (MPa)	CRank	CType	TRank	TType
Kz	3.72	1275	28.61	4	1	5	1
La	1.70	1921	8.67	3	0	5	1
Lb	1.13	1174	9.46	6	0	5	1
Lc	0.61	2439	2.44	4	1	6	1
Ld	1.95	3361	5.69	4	1	2	0
Le	4.94	2588	18.72	6	1	4	1
Lf	1.41	4286	3.23				
Lg	0.61	4192	1.42	5	1	5	1
Lh	0.31	2890	1.06	6	0	4	0
Li	1.15	2837	3.98	3	1	6	0
Lj	1.44	689	20.54	6	0	2	0
Lk	1.63	2602	6.14	5	1	3	0

Unbleached Kraft Pulp (Treated with D/S) Data (ADS)

Mount	Load (g)	Area (μm^2)	BondStr (MPa)	CRank	CType	TRank	TType
Qz	0.74	1412	5.15	5	1	5	1
Ra	1.98	1748	11.12	4	1	3	1
Rb	0.30	1996	1.47	3	1	5	1
Rc	0.95	2657	3.51	4	1	5	1
Rd	1.67	1934	8.48	3	1	4	1
Re	1.48	3286	4.43	5	0	5	0
Rf	1.98	1439	13.50	5	1	5	1
Rg	0.47	786	5.83	4	0	4	0
Rh		3681				5	0
Ri	1.63	3804	4.19	5	1	4	0
Rj	1.48	2500	5.81	5	1	5	1
Rk	0.35	3452	1.00	3	0	5	0
Rl	2.72	1843	14.46	3	1	4	1
Rm	2.05	1730	11.61	2	1	4	1
Rn	2.45	1516	15.85	5	1	5	1
Ro	1.17	2199	5.25	5	1	5	1
Rp	1.64	1448	11.08	4	1	5	1
Rq	2.18	1450	14.75	3	1	5	1
Rr	1.99	2107	9.24	4	1	5	1
Rs	1.73	2026	8.37	3	0	5	0
Rt	1.67	2119	7.71	6	1	5	1
Ru	3.60	1218	28.99	3	1	5	1
Rv	0.27	1639	1.60	2	0	4	1
Rw	1.51	3134	4.73				
Rx	1.43	1835	7.64	5	1	6	1
Ry	0.31			3	1	4	1
Rz	0.91	1627	5.47	4	1	4	1
Sa		1723					
Sb	0.15	2252	0.67	5	1	3	0
Sc	0.83	3289	2.48			5	0
Sd	0.18	157	10.99	5	1	6	1
Se	0.59	1736	3.31	3	0	5	1
Sf	1.20	3643	3.23	2	1	3	0
Sg	1.99	1712	11.40	4	1	5	1
Sh	0.78	1926	3.97	4	1	4	1
Si	1.95	1641	11.63	5	1	2	0

Unbleached Kraft Pulp (Treated with D/S) Data (ADS) (Continued)

Mount	Load (g)	Area (μm^2)	BondStr (MPa)	CRank	CType	TRank	TType
Sj	0.45	1391	3.16	4	0	3	0
Sk	2.68	2536	10.36	5	0	5	0
Sl	0.86	2260	3.71	5	1	5	1
Sm	3.28	1982	16.21	4	1	6	0
Sn	0.87	1738	4.92			5	1
So	1.83	1736	10.35	3	1	5	0
Sp	3.33	2333	14.00	5	0	5	1
Sq	0.99	1690	5.74	4	0	5	1
Sr	1.73	1797	9.45	4	1	6	1
Ss	3.78	1920	19.31	5	1	5	1
St	1.77	2052	8.45	5	1	6	1
Su	1.46	1700	8.43	5	1	5	1

Unbleached Kraft Pine Data (75% RH) (A75)

Mount	Load (g)	Area (μm^2)	BondStr (MPa)	CRank	CType	TRank	TType
Xl	0.69	2542	2.64	3	1	3	1
Xm	0.95	4425	2.10	4	0	4	0
Xn	1.59	1671	9.34	6	1	4	1
Xo	0.59	2624	2.21	5	1	4	1
Xp	1.36	3261	4.08	5	1	2	1
Xq	0.25	3077	0.80	4	1	4	1
Xs	0.91	1206	7.37	4	1	3	0
Xu	0.13	2313	0.54	4	1	3	1
Xv	0.26	3108	0.81	3	0	2	1
Xw	0.25	964	2.54	1	0	2	0
Xx	0.85	2251	3.70	2	0	4	0
Xy	0.57	3428	1.64	5	1	4	1
Xz	0.44	1283	3.39	5	1	4	1
Ya	0.52	1835	2.79	4	1	3	1
Yb	0.70	1823	3.75	4	1	6	1
Yc	0.64	1965	3.22	2	0	2	0
Yd	0.28	2231	1.23	3	1	4	1
Ye	0.13	1616	0.76	4	1	4	1
Yf	0.12	1628	0.74	5	1	4	1
Yg	0.35	2770	1.25	3	1	3	0
Yh	0.20	2760	0.72	2	0	4	1
Yi	0.84	2550	3.24	4	1	2	0
Yj	0.18	2280	0.76	5	1	3	0
Yl	0.11	1181	0.88	6	1	4	1
Ym	0.62	2691	2.25	4	0	4	1
Yn	0.24	3884	0.60	5	1	4	0
Yp	0.44	2702	1.58	3	1	4	1
Yq	0.20	2317	0.85	4	0	3	0
Yr	0.21	1572	1.30	5	1	5	1
Ys	1.47	1852	7.77	5	1	6	1
Yt	0.23	982	2.30	4	1	3	1
Yu	0.47	2001	2.32	4	1	4	1
Yv	0.95	2952	3.16	2	1		
Yx	0.05	1881	0.26	2	0	2	0
Yy	0.96	1883	4.99	3	1	4	1
Yz	0.51	744	6.66	3	1	5	1

Unbleached Kraft Pine Data (75% RH) (A75) (Continued)

Mount	Load (g)	Area (μm^2)	BondStr (MPa)	CRank	CType	TRank	TType
Za	1.59	1820	8.57	4	1	6	1
Zb	1.02	3351	2.99	6	0	4	1
Zc	0.26	2738	0.94	4	0	4	0
Zd	0.89	3106	2.80			4	0
Ze	0.62	2411	2.51	4	1	4	1
Zf	2.03	2269	8.77	6	1	4	1
Zg	0.28	1298	2.11	3	1	4	1

Unbleached Kraft Pulp (88% RH) Data (A88)

Mount	Load (g)	Area (μm^2)	BondStr (MPa)	CRank	CType	TRank	TType
Ur	0.17	4225	0.39	3	0	2	0
Us	1.61	1885	8.39	6	1	4	1
Ut	0.27	4000	0.65	1	0	3	1
Uu	0.27	3105	0.84	4	1	3	0
Uv	0.38	2532	1.46	4	0	2	0
Uw	0.20	2079	0.94	4	1	3	1
Ux	0.39	1650	2.30	5	1	4	1
Uz	0.47	2623	1.74	3	1		
Va	0.41	2197	1.85	5	1	3	1
Vb	0.09	1964	0.47	5	0	2	0
Vc	0.52	1556	3.26	3	1	3	1
Vd	0.50	824	5.98	3	1	3	1
Ve	0.15	2338	0.63	6	1	2	0
Vf	0.16	2494	0.62	2	0	2	0
Vg		2748		4	1	4	1
Vh	0.36	2299	1.54	3	0	4	0
Vi	0.26	1481	1.75	3	1	4	1
Vj	0.40	1480	2.65			4	1
Vk	0.40	2364	1.64	4	1	3	0
Vl	0.57	1297	4.28	3	1	3	1
Vm	0.40	2262	1.74	2	0	5	1
Vn	0.35	1492	2.29	3	1	3	1
Vo	1.47	1827	7.89	5	1	3	0
Vp	0.07	2751	0.26	3	0	4	1
Vq	0.25	2077	1.17	4	1	2	1
Vr	0.40	1948	2.00	4	1	3	1
Vs	0.06	1209	0.52	5	1	4	1
Vt	0.11	2330	0.45	2	0	3	0
Vu	0.84	4477	1.83	3	0	3	1
Vw	0.38	2034	1.82	4	1	3	1
Vx	0.19	1407	1.33			4	1
Vy	0.49	1493	3.22	4	1	3	1
Vz	0.18	3401	0.52	3	0	3	0
Wa	0.19	2244	0.83	5	1	5	1
Wb	0.80	1818	0.43	3	1	3	1
Wc	0.30	2298	1.29	5	1	5	1

Unbleached Kraft Pulp (88% RH) Data (A88) (Continued)

Mount	Load (g)	Area (μm^2)	BondStr (MPa)	CRank	CType	TRank	TType
Wd	0.74	1257	5.76	6	1	3	1
We	0.72	1382	5.08	4	1	5	1
Wf	0.57	1941	2.86	3	0	4	1
Wg	0.47	1901	2.42	5	1	3	1
Wh	0.73	2088	3.44			4	1
Wi	0.16	3342	0.47	4	1	4	1
Wj	0.24	3839	0.60			2	0
Wl	0.21	2256	0.90	4	1	4	1
Wm	0.37	1732	2.12	4	1	4	1

Unbleached Kraft Pulp (Beaten to 345 mL CSF) Data (A3)

Mount	Load (g)	Area (μm^2)	BondStr (MPa)	CRank	CType	TRank	TType
Sv	0.52	1793	2.86	4	1	4	1
Sw	1.99	742	26.30	5	1	3	1
Sx	0.16	846	1.89	6	1	4	1
Sy	0.96	2068	4.54			3	1
Sz	0.41	719	5.56			4	1
Ta	0.86	2212	3.82	4	1	4	0
Tb	0.42	1479	2.77	5	1	4	1
Tc	0.19	3287	0.57	3	1	3	0
Td	0.48	2496	1.90	4	1	3	1
Te	1.16	1838	6.16	5	1	4	1
Tf	1.08	2463	4.29			6	1
Th	0.83	2024	4.03	3	1	3	0
Ti	0.84	2226	3.68	4	1	4	1
Tj	0.25	1425	1.70			3	0
Tk	0.93	5649	1.61	4	0	3	0
Tm	0.96	2580	3.65	4	1	5	1
Tn	0.19	2447	0.78	3	1	4	1
To	2.48	1875	12.97	3	1		
Tp	0.51	1619	3.11			3	1
Tq	0.32	1111	2.80	5	1	5	1
Tr	0.77	1779	4.23	6	1	5	1
Ts	0.94	3536	2.61	6	1	5	1
Tt	1.61	1380	11.43	3	1	5	1
Tu	0.16	1203	1.29	4	1	4	1
Tv	0.49	805	5.93	3	1	3	1
Tw	0.42	2824	1.45	5	1	4	1
Tx	0.61	2633	2.25	5	1	3	0
Ty	0.60	2861	2.06	5	1	5	1
Tz	0.56	2181	2.53	5	1	4	1
Ua	0.18	3672	0.48	5	1	4	1
Ub	1.07	2958	3.55	5	1	5	1
Uc	0.40	1992	1.97	4	1	3	0
Ud	1.19	4046	2.88	6	0	4	0
Ue	0.58	1406	4.06	5	1	4	1
Ug	0.77	1967	3.85	5	1	5	1
Uh	0.42	4351	0.95	3	1	3	1

Unbleached Kraft Pulp (Beaten to 345 mL CSF) Data (A3) (Continued)

Mount	Load (g)	Area (μm^2)	BondStr (MPa)	CRank	CType	TRank	TType
Uj	0.29	2714	1.06	5	1	5	1
Uk	0.15	738	1.99	5	1	4	1
Ul	0.51	3816	1.31	4	1	4	1
Um	0.94	2437	3.76	5	1	4	1
Un	0.17	1832	0.89	4	0	3	1
Uo	0.26	2231	1.15	4	1	4	1
Up	0.57	3894	1.43	4	1	5	1
Uq	0.83	2790	2.91	4	1	4	1

TMP Data (T0)

Mount	Load (g)	Area μm²)	BondStr (MPa)	CRank	CType	TRank	TType
Nh		488		2	0	5	1
Nj	0.90	1854	4.76	2	0	3	1
Nk	0.47	1860	2.46			3	1
Nl	0.28	1680	1.65	3	0	4	0
Nm	0.13	1309	1.00	3	0	2	0
No	1.00	1456	6.72	3	1	4	1
Np	0.58	1523	3.72	3	0	2	1
Nq	0.10	200	4.80				
Nr		348		3	0	3	1
Ns		1060		4	0	3	0
Nt	0.07	250	2.82	3	1	3	1
Nu	0.06	359	1.58	3	1	3	1
Nv	1.88	1735	10.61	6	0	3	1
Nw	0.35	1049	3.27	3	1	4	1
Nx	0.13	1445	0.90	3	1	3	0
Ny	0.06	449	1.33	3	1	4	1
Nz	0.35	1628	2.11	2	0	3	1
Oa	0.34	1865	1.78	2	0	3	1
Ob	0.59	476	12.24	3	1	3	1
Oc	0.77	570	13.18	2	0	3	1
Od	0.35	1196	2.88	2	0	2	1
Oe	0.03	1153	0.28			3	1
Of	0.67	855	7.65	4	0	3	0
Og	0.63	260	23.72	4	1	3	1
Oh	0.93	408	22.30			3	1
Oi	0.20	439	4.42	3	1	4	0
Oj	0.13	34	37.39	3	1	3	1
Ok	0.25	147	16.70	4	1	3	1
Ol	0.38	414	9.11			2	1
Om	0.21	317	6.46	4	1	4	1
On	0.04	181	2.39	4	0	3	1
Oo	0.07	279	2.53	3	0	4	1
Oq	0.27	840	3.11			3	1
Or	0.57	757	7.44	4	1	2	1
Ot	0.15	624	2.36	3	1	2	0
Ou	0.57	347	16.18	4	1	3	1

TMP Data (T0) (Continued)

Mount	Load (g)	Area (μm^2)	BondStr (MPa)	CRank	CType	TRank	TType
Ov	0.46	563	8.04	3	1	2	1
Ow	0.86	221	38.24	2	1	3	1
Ox	0.12	723	1.61			2	0
Oy	0.60	497	11.78	4	1	2	0
Oz	0.02	45	3.90	4	1		
Pa	0.16	163	9.70	4	0	3	1
Pb	0.51	599	8.31	3	0	4	1
Pc	0.34	795	4.18	3	1	3	1

TMP (Treated with A/C) Data (TAC)

Mount	Load (g)	Area (μm^2)	BondStr (MPa)	CRank	CType	TRank	TType
Pd	1.88	2130	8.63	3	1	3	1
Pe	0.65	1771	3.59	6	1	6	1
Pf	0.99	1062	9.14	4	1	4	1
Pg	0.79	1333	5.82	3	1	4	1
Ph	0.34	140	24.2	3	1	3	1
Pi	0.34	1165	2.89	3	1	3	1
Pj	0.74	1718	4.22	5	0	4	1
Pk	0.34	451	7.30	6	0	3	0
Pl	1.19	1693	6.87	4	0	6	0
Pm	0.42	1454	2.86	4	1	3	1
Pn	1.60	3535	4.45	2	1	3	0
Po	1.72	2256	7.48	5	1	5	1
Pp	1.19	2841	4.09	5	0	3	0
Pq	0.59	1209	4.79	4	1	4	1
Pr	1.50	3028	4.85	4	1	3	1
Ps	1.08	1412	7.48	3	1	3	0
Pt	0.90	1256	7.05	4	1	4	1
Pu	0.90	1289	7.22	5	1	5	1
Pv	2.06	3375	5.97	5	1	5	1
Pw	1.16	2462	4.63	6	1	6	1
Px	5.66	1406	39.5	5	1	3	0
Py	1.51	1276	11.6	6	1	5	1
Pz	0.85	1889	4.42	4	1	3	0
Qa	0.23	808	2.80	3	1	4	1
Qb	2.01	1666	11.8	4	1	5	0
Qc	1.76	1042	16.5	4	0	4	1
Qd	1.95	1739	11.0	3	0	4	1
Qe	1.54	1603	9.42			4	1
Qf	0.87	2142	3.97	4	0	5	1
Qg	2.59	1972	12.9	4	1	4	1
Qh	1.52	1672	8.92	6	0	4	1
Qi	1.61	857	18.4	3	1	4	1
Qj	0.55	1079	5.02	4	1	5	1
Qk	1.01	2101	4.71	4	1	4	1
Ql	1.95	1686	11.4	3	1	4	1
Qm	0.41	1511	2.66	4	1	5	1

TMP (Treated with A/C) Data (TAC) (Continued)

Mount	Load (g)	Area (μm^2)	BondStr (MPa)	CRank	CType	TRank	TType
Qn	1.37	2627	5.10	6	0	5	1
Qo	1.39	232	58.9	4	1	3	1
Qp	0.79	896	8.64	5	0	6	1
Qq	2.15	1957	10.8	5	1	5	1
Qr	0.97	2058	4.60	5	1	5	1
Qs	1.68	446	36.9	6	0	6	0
Qt	1.29	2616	4.85	4	1	4	1
Qu	1.49	2283	6.41	3	0	5	0
Qv	0.72	269	26.3	5	0	5	1
Qw	1.33	1838	7.11	6	1	5	1
Qx	0.23	1068	2.14	5	1	5	1
Qy	1.39	1601	8.53	4	1	3	1